Summer 2000

Reduction of peak to average power ratio in OFDM and OFDM-CDMA system

Jie Cheng
New Jersey Institute of Technology

ABSTRACT

REDUCTION OF PEAK TO AVERAGE POWER RATIO IN OFDM AND OFDM-CDMA SYSTEM

by
Jie Cheng

High Peak to Average Power Ratio is a main problem in Orthogonal Frequency Division Multiplexing(OFDM) system and Orthogonal Frequency Division Multiplexing - Code Division Multiple Access (OFDM-CDMA) system. Considering a compensated High Power Amplifier(HPA), in order to keep linearity for amplification, Input Back-Off(IBO) of the HPA has to be increased for handling a high PAPR. Higher IBO will make HPA less efficient. Additionally, a signal with high PAPR will suffer clipping when PAPR is larger than IBO of the HPA. Clipping can cause the distortion of the signal and deteriorate the performance of the system. Reduction of PAPR is a main issue for OFDM and OFDM-CDMA application. In this thesis, some coding schemes are discussed to reduce PAPR. Of all possible code words for transmission, some code words with lower PAPR are chosen for transmission. Some redundancies are added to the end of the original code words to form these lower PAPR code words, though the net bit rate will decrease as a tradeoff. To reduce PAPR block coding scheme and cyclic coding scheme are discussed first. An odd parity bit is added as a redundancy bit. Also the code rate is 3/4. A novel block coding scheme with bit position control is discussed, where the position of the redundancy bit in the original code words is chosen by a feedback selection. For multiuser application, OFDM-CDMA is discussed. Walsh-Hadard(WH) and Complementary(CP) and Gold code sequences are used as the spreading sequences. These coding schemes used in OFDM system are also used before spreading to reduce PAPR in OFDM-CDMA system.

REDUCTION OF PEAK TO AVERAGE POWER RATIO IN OFDM AND OFDM-CDMA SYSTEM

by
Jie Cheng

A Thesis
Submitted to the Faculty of
New Jersey Institute of Technology
in Partial Fulfillment of the Requirements for the Degree of
Master of Science in Electrical Engineering

Department of Electrical and Computer Engineering

August 2000

APPROVAL PAGE

REDUCTION OF PEAK TO AVERAGE POWER RATIO IN OFDM AND OFDM-CDMA SYSTEM

Jie Cheng

Dr. Yeheskel Bar-Ness, Thesis Advisor   Date
Distinguished Professor of Electrical and Computer Engineering, NJIT

Dr. Alexander Haimovich, Committee Member   Date
Associate Professor of Electrical and Computer Engineering, NJIT

Dr. Haibin Zhu, Committee Member   Date
Visiting Professor of Computer and Information Science, NJIT

BIOGRAPHICAL SKETCH

Author: Jie Cheng

Degree: Master of Science

Date: August 2000

Undergraduate and Graduate Education:

- Master of Science in Electrical Engineering,
  New Jersey Institute of Technology, Newark, NJ, 1998

- Bachelor of Science in Electrical Engineering,
  Xidian University, Xi'an, China, 1994

Major: Electrical Engineering

This thesis is dedicated to my family

ACKNOWLEDGMENT

I would like to express my sincere gratitude to my advisor, Dr. Yeheskel Bar-Ness. I must thank deeply for his kind assistance, guidance throughout the writing of this thesis.

I would also like to thank Dr. Alexander Haimovich and Dr. Haibin Zhu for serving as members on the thesis committee and for their valuable advice.

I would also like to thank my colleagues at the Center for Communications and Signal Processing Research at NJIT for their friendship and good suggestion.

Most of all, I sincerely thank my parents, my wife and my brother for their constant support and encouragement.

TABLE OF CONTENTS

LIST OF TABLES

LIST OF FIGURES

CHAPTER 1

INTRODUCTION

In this thesis, Reduction of Peak to Average Power Ratio(PAPR) in OFDM and OFDM-CDMA system is discussed.

Multicarrier transmission scheme such as OFDM (Orthogonal Frequency Division Multiplexing) has been proposed for many different types of systems such as DAB (Digital Audio Broadcasting) and radio LANs(Local Area Networks). [1, 2] The principle of multicarrier transmission is simple, that is, instead of transmitting at a high transmission rate on a single carrier, transmitting at a low transmission rate on multiple carriers, at the same time, the net bit rate is not changed. In OFDM system, for the transmission bit rate is R_b, the bit duration time is $T_b = \frac{1}{R_b}$. Using to a Serial to Parallel converter, a block of N data bits is converted into a parallel form with the time duration $T_d = NT_b$. Therefore, the transmission rate is decreased to $R_d = \frac{1}{NR_b}$. Then an IFFT(Inverse Fast Fourier Transform) is used for multi-carrier modulation. A block of data is mapped into each subcarrier. Subcarriers are orthogonal to each other while the frequency spectrum overlaps.

The mobile communication channel can be classified using coherent bandwidth B_x and the coherent time T_x. The relation between the coherent bandwidth and the multipath spread τ is $B_x = \frac{1}{2\pi\tau}$. The relation between the coherent time and the Doppler spread B_d is $T_x = \frac{1}{B_d}$. If the transmission rate R_b is larger than the channel coherent bandwidth, then the transmitted signal will suffer frequency selective fading. In OFDM system, the transmitted rate R_d is decreased enough to be sufficiently less than the coherent bandwidth B_x, so the channel can be assumed as a frequency non-selective channel, that is, non-time dispersive channel. In addition, the time duration T_d is less than the coherent time T_x, so the doppler spread is ignored. The channel is no time selective or non-frequency dispersion channel.

However, one of the main disadvantages of OFDM system is high Peak to Average

Power Ratio(PAPR). Considering symbols with BPSK modulation, when the phase of different subcarriers is the same, the different subcarrier components of the signal will be added together to a peak value, so high PAPR is produced. It can be calculated that the peak power value for N subcarriers is N^2, and PAPR for N subcarriers is N. High PAPR will highly deteriorate the efficiency of the High Power Amplifier(HPA). There are two typical models for HPA in this thesis. One is Travelling Wave Tube Amplifier(TWTA), the other is Solid State Power Amplifier(SSPA). Using predistortion technique to compensate for the nonlinearity of HPA, HPA can be assumed a compensated linear HPA. That is, when the peak of the signal is lower than the saturation amplitude of HPA, it keeps linearity; otherwise, the amplitude of the signal is clipped to the saturation amplitude. Clipping causes signal distortion and spectral spreading. In OFDM system, because of high PAPR, Input BackOff(IBO) of HPA has to be increased to alleviate the clipping effect. However, high IBO will make HPA less efficient.

Many schemes have been proposed to reduce PAPR in OFDM system. Among these is scheme which uses amplitude limiting at the point of generation [3] or coding [3, 4, 5, 6]. Amplitude limiting leads to an increase of the bit error rate(BER), while coding schemes will decrease the net bit rate. Block coding scheme, proposed by A.E.Jones [4, 7], is suitable when the number of subcarriers is small. Golay complementary sequences have been proposed recently in [8, 9, 10]. The main problem for this scheme is that the rate (in the order of $ln(N)/N$) becomes small when the number of N of the subcarriers is large. In the traditional block coding scheme, one odd parity bit is added at the end of the code word, thus only part of all possible code words are used for OFDM modulation. Simulation results show that when the number of subcarriers N is small, this is an effective method, however, when N is large, only little PAPR reduction is obtained. In this thesis, a novel block coding scheme with bit position control is used for the PAPR reduction. It

results in an improvement in PAPR reduction. With this scheme, first the code word is divided into small blocks of code words. Then the odd parity bit for each small code word is produced. That is with in this scheme, the odd parity bit can be inserted in any position of the code word instead of the end of the code word. It would be shown that inserting the redundancy bit into different position of the original code word can produce different PAPR. A Code Word Selector is used to select a specific code word with the lowest PAPR for transmission. Clearly the position information of the odd parity bits are also transmitted as side information for decoding. The simulation results show that this novel block coding scheme can reduce PAPR significantly better than these using previous block coding schemes.

OFDM-CDMA(Orthogonal Frequency Division Multiplexing - Code Division Multiple Access) is another interesting field for multicarrier application [11, 12]. OFDM-CDMA is a combination of DS-CDMA and OFDM. Therefore OFDM-CDMA inherits all the bad traits as well as good traits from their parents. OFDM-CDMA also suffer the high PAPR problem. For N subcarrier system, PAPR is also N as in single user case.

DS-CDMA(Direct Sequence-CDMA) is a method to share spectrum among multiple simultaneous users and it can exploit frequency diversity using RAKE receivers. However, in a time dispersive channel, high intersymbol interference (ISI) will deteriorate the system performance with a large spread factor N. Unlike DS-CDMA, OFDM-CDMA applies spreading sequences in frequency domain. The original information becomes spread in frequency domain directly. As a result of this, the signal can overcome the time delay spread of the time dispersive channel. In this thesis, Walsh-Hadamard(WH), complementary(CP) sequences and gold code are used for spreading sequences. In OFDM-CDMA system, spreading sequences are used to distinguish data from different users. Using OFDM modulation, each chip of the spreading sequence is mapped to different subcarrier. Compared with

OFDM, OFDM-CDMA spreads an information bit over many subcarriers, so it can make use of information contained in sound subcarriers through the fading channel to recover the original symbol.

This thesis is organized as follows. In Chapter 2, an OFDM system model is discussed first. PAPR in OFDM system is defined and some characteristics of PAPR are also discussed. Some block coding schemes are used for PAPR reduction. Finally a novel block coding scheme with bit position control is proposed and some simulation results are given for comparison. In Chapter 3, the communication channel is classified and discussed. The characteristics of the channel are also discussed. In Chapter 4, OFDM-CDMA system model is discussed and PAPR reduction using the previously proposed block coding schemes and the novel block coding with bit position control in OFDM-CDMA system is simulated and compared.

CHAPTER 2

ORTHOGONAL FREQUENCY DIVISION MULTIPLEXING

2.1 Introduction

Orthogonal Frequency Division Multiplexing(OFDM), a special form of Multi-Carrier Modulation(MCM) with densely spaced subcarriers and overlapping spectra was patented in the U.S. in 1970 [13]. OFDM abandoned the use of steep bandpass filters that completely separated the spectrum of individual subcarriers,which is commonly applied in Frequency Division Multiple Access(FDMA) systems. In OFDM system, the serial input data are first passed through a serial-to-parallel converter. the parallel data are mapped into each subcarrier. Thus, they become the frequency domain symbols. To get the time domain data again, an Inverse Discrete Fourier Transform or its fast version, IFFT, is applied. These subcarriers are orthogonal to each other while the frequency spectrum overlaps. The frequency spacing between the subcarrier is minimum in OFDM. This gives OFDM high spectral efficiency. OFDM also has some disadvantages, such as sensitivity to frequency offset and high Peak to Average Power Ratio(PAPR). In this chapter, the PAPR in OFDM system is discussed and some coding techniques for PAPR reduction are proposed.

2.2 OFDM System Model

The OFDM system model is shown in figure 2.1. The encoder is used to choose the possible code words with lower PAPR. IFFT block is used for multicarrier modulation. For transmission, High Power Amplifier(HPA) has to be included. In order to reduce the influence of the nonlinearity of HPA, the predistortion block is also included in this system. Thus, HPA for the transmitted signal can be considered as a compensated HPA [14, 15]. In the receiver, FFT block is used for multicarrier

5

demodulation. The decoder and the detector are also included for the recovery of the transmitted signal.
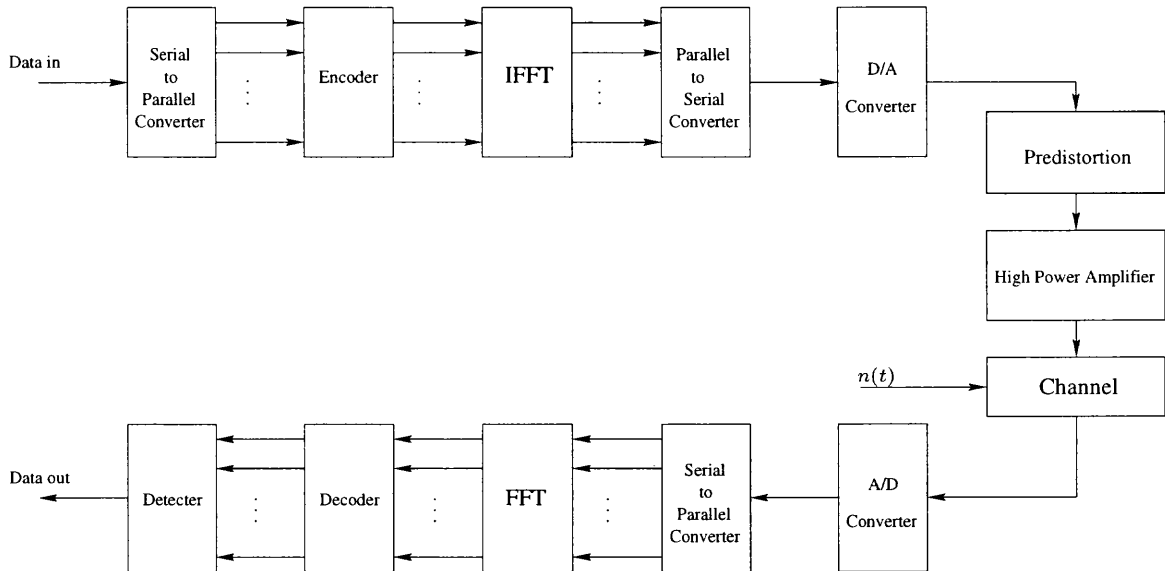
Figure 2.1 Block Diagram of OFDM System

2.2.1 Transmitter Model

In OFDM transmitter shown in figure 2.2 , the input data is a serial sequence $d(0), d(1), \ldots, d(N-1)$ with the time duration T_d. After a serial to parallel converter, that block data is converted into a parallel form with time duration NT_d. In Figure 2.2, the encoder is not included. Each symbol of one data block is mapped to the corresponding carrier. Thus, they become frequency domain symbols, that is, $s(0), s(1), \ldots, s(N-1)$. After a parallel to serial converter and D/A converter, the output of the transmitter is

$$S(t) = \sum_{n=0}^{N-1} d(n)e^{j(2\pi f_n t + \beta_n)} \tag{2.1}$$

where the input data $d(n)$ is modulated by Binary Phase Shift Keying(BPSK), and it is assumed to be either 1 or −1 with the same probability. f_n is the carrier frequency for $d(n)$ and β_n is the initial phase of the nth carrier. For simplicity, the initial phase

$\beta_n = 0$. Choosing $f_n = \frac{n}{NT_d}$, then the discrete form of $S(t)$ is

$$s(kT_d) = \sum_{n=0}^{N-1} d(n)e^{j2\pi \frac{n}{NT_d}kT_d} \tag{2.2}$$

that is

$$\begin{aligned} s(k) &= \sum_{n=0}^{N-1} d(n)e^{j2\pi \frac{nk}{N}} \\ &= IFFT\{d(n)\} \end{aligned} \tag{2.3}$$
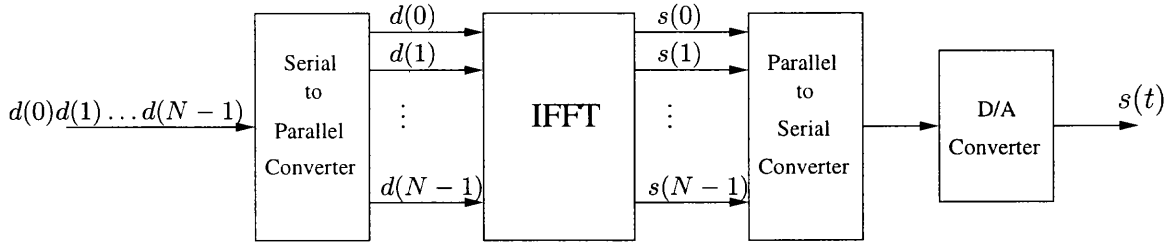
Figure 2.2 Block Diagram of OFDM Transmitter

2.2.2 Receiver Model

Suppose the channel model in time domain is $h(n)$, correspondingly, in the form in frequency domain, we have

$$\begin{aligned} H(k) &= FFT\{h(n)\} \\ &= \sum_{n=0}^{N-1} h(n)e^{-j2\pi \frac{nk}{N}} \end{aligned} \tag{2.4}$$

Ignoring the noise influence, the discrete form of the received signal $r(n)$ can be expressed as (see Figure 2.3)

$$\begin{aligned} r(n) &= s(n) * h(n) \\ &= \sum_{m=0}^{N-1} s(m)h(n-m) \\ &= \sum_{m=0}^{N-1}[\sum_{p=0}^{N-1} d(p)e^{j2\pi \frac{pm}{N}}]h(n-m) \end{aligned}$$
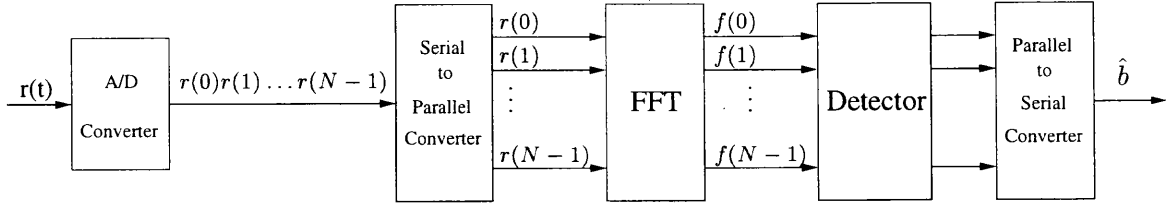
Figure 2.3 Block Diagram of OFDM Receiver

$$
\begin{aligned}
&= \sum_{p=0}^{N-1} d(p)[\sum_{m=0}^{N-1} e^{j2\pi \frac{pm}{N}} h(n-m)] \\
&= \sum_{p=0}^{N-1} d(p)[e^{j2\pi \frac{pm}{N}} * h(m)] \\
&= \sum_{p=0}^{N-1} d(p)[\sum_{m'=0}^{N-1} e^{j2\pi \frac{p(n-m')}{N}} h(m')] \\
&= \sum_{p=0}^{N-1} d(p)e^{j2\pi \frac{pn}{N}}[\sum_{m'=0}^{N-1} h(m')e^{-j2\pi \frac{pm'}{N}}] \\
&= \sum_{p=0}^{N-1} d(p)H(p)e^{j2\pi \frac{pn}{N}} \\
&= IFFT[d(p)H(p)] \qquad (2.5)
\end{aligned}
$$

Thus, the output of the FFT block at the receiver is

$$
\begin{aligned}
f(p) &= FFT[r(n)] \\
&= FFT\{IFFT[d(p)H(p)]\} \\
&= d(p)H(p) \qquad (2.6)
\end{aligned}
$$

Then a detector is used to estimate the transmitted data. After that, a parallel to serial converter is used to get the resultant serial sequence $\hat{b}$.

$$
\hat{b} = sign(f(p) + \xi(p)) \qquad (2.7)
$$

Where $\xi(p)$ is the Gaussian noise. The receiver model is shown in 2.3.

2.3 Peak to Average Power Ratio in OFDM System

2.3.1 Definition

OFDM, like other forms of multicarrier modulation system, has a main disadvantage, high peak to average power ratio(PAPR) of the transmitted signal $S(t)$ [16, 17]. PAPR of a signal is a very important parameter, because it determines the input backoff factor of the amplifier to avoid clipping and spectral regrowth.

Here, the definition of PAPR [4] is

$$PAPR = \frac{max\{|S(t)|^2\}|_{t\in[0,T]}}{\frac{1}{T}\int_0^T |S(t)|^2\,dt} \tag{2.8}$$

where $S(t)$ is given in Equation (2.1).

2.3.2 Analysis of PAPR in OFDM

In this section, some characteristics of PAPR defined in Equation (2.8) are discussed.

1. First it is shown that the average power of the signal $s(t)$ is the length of the code word N. In fact, by definition the average power of the signal $S(t)$ is

$$
\begin{aligned}
\text{avg}[S(t)] &= \frac{1}{T}\int_0^T |S(t)|^2\,dt \\
&= \frac{1}{T}\int_0^T |\sum_{n=0}^{N-1} d(n)e^{j2\pi\frac{n}{NT_d}t}|^2\,dt \\
&= \frac{1}{T}\int_0^T (\sum_{n=0}^{N-1} d(n)\cos(2\pi\frac{n}{NT_d}t))^2 + (\sum_{n=0}^{N-1} d(n)\sin(2\pi\frac{n}{NT_d}t))^2\,dt \\
&= \frac{1}{T}\int_0^T \sum_{n=0}^{N-1} d^2(n)\cos^2(2\pi\frac{n}{NT_d}t) + \sum_{n=0}^{N-1} d^2(n)\sin^2(2\pi\frac{n}{NT_d}t) \\
&\quad + \sum_{n\neq m} 2d(n)d(m)\cos(2\pi\frac{n}{NT_d}t)\cos(2\pi\frac{m}{NT_d}t) + \\
&\quad \sum_{n\neq m} 2d(n)d(m)\sin(2\pi\frac{n}{NT_d}t)\sin(2\pi\frac{m}{NT_d}t)\,dt
\end{aligned}
$$

$$\tag{2.9}$$

Consider $d(n)$ is a BPSK symbol, so $|d(n)| = 1$ when $t \in [0, T]$, and $T = NT_d$, thus

$$\frac{1}{T} \int_0^T \sum_{n \neq m} 2d(n)d(m) \cos(2\pi \frac{n}{NT_d}t) \cos(2\pi \frac{m}{NT_d}t) \, dt$$

$$+\frac{1}{T} \int_0^T \sum_{n \neq m} 2d(n)d(m) \sin(2\pi \frac{n}{NT_d}t) \sin(2\pi \frac{m}{NT_d}t) \, dt$$

$$= \frac{2}{T} \sum_{n \neq m} d(n)d(m) \int_0^T \cos \frac{2\pi(n-m)}{NT_d} \, dt$$

$$= 0$$

The average power of the signal $S(t)$ is

$$\begin{aligned}
\text{avg}[S(t)] &= \frac{1}{T} \int_0^T (\sum_{n=0}^{N-1} d^2(n)) \, dt \\
&= N\frac{1}{T} \int_0^T d^2(n) \, dt \\
&= N \quad\quad\quad\quad\quad\quad (2.10)
\end{aligned}$$

Because the average power of $S(t)$ is constant, in order to decrease PAPR, the maximum of of the instanteous signal power $|S(t)|^2$ should be decreased.

2. It is shown that the complementary of a code word has the same PAPR as the original one for BPSK modulation.

If a code word c is reprented as a vector $[\lambda_0, \lambda_1, \dots, \lambda_{N-1}]$, then the code word $\bar{c}$, the complementary of c can be represented as a vector $[\lambda_0+\pi, \lambda_1+\pi, \dots, \lambda_{N-1}+\pi]$ for BPSK modulation. To Calculate the $PAPR_c$ for c and $PAPR_{\bar{c}}$ for $\bar{c}$, first calculate the instantenous amplitude of $S(t)$. For code word c, the amplitude is

$$|S_c(t)| = |\sum_{n=0}^{N-1} e^{j\frac{2\pi n}{N}\frac{t}{T_d}} e^{j\lambda_n}| \quad\quad\quad\quad (2.11)$$

For code word $\bar{c}$, the amplitude is

$$|S_{\bar{c}}(t)| = |\sum_{n=0}^{N-1} e^{j\frac{2\pi n}{N}\frac{t}{T_d}} e^{j(\lambda_n+\pi)}|$$

$$
\begin{aligned}
&= \ \left| \sum_{n=0}^{N-1} e^{j\frac{2\pi n}{N}\frac{t}{T_d}} e^{j\lambda_n} \right| \times \left| e^{j\pi} \right| \\
&= \ |S_c(t)| \tag{2.12}
\end{aligned}
$$

Thus, the amplitude is the same for c and $\bar{c}$. Using Equation (2.8) The PAPR is also the same for c and $\bar{c}$.

3. If for the code word c is $[c_0, c_1, \cdots, c_{N-1}]$, the order of these bits from the first bit to the last bit is reversed, then the resultant code word is $\hat{c}$ is $[c_{N-1}, \cdots, c_1, c_0]$. It can be proved that c and $\hat{c}$ have the same PAPR.

For code word $\hat{c}$, the amplitude is

$$
\begin{aligned}
|S_{\hat{c}}(t)| &= \ \left| \sum_{n=0}^{N-1} e^{j\frac{2\pi(N-1-n)}{N}\frac{t}{T_d}} e^{j\lambda_n} \right| \\
&= \ \left| e^{j\frac{2\pi(N-1)t}{NT_d}} \sum_{n=0}^{N-1} e^{j\frac{2\pi(-n)}{N}\frac{t}{T_d}} e^{j\lambda_n} \right| \\
&= \ \left| e^{j\frac{2\pi(N-1)t}{NT_d}} \right| \times \left| \sum_{n=0}^{N-1} e^{j\frac{2\pi(-n)}{N}\frac{t}{T_d}} e^{j\lambda_n} \right| \\
&= \ \left| \sum_{n=0}^{N-1} e^{j\frac{2\pi(-n)}{N}\frac{t}{T_d}} e^{j\lambda_n} \right| \\
&= \ \left| \sum_{n=0}^{N-1} e^{j\frac{2\pi n}{N}\frac{t}{T_d}} e^{j(-\lambda_n)} \right| \tag{2.13}
\end{aligned}
$$

As a conjugate term. For the case of BPSK, $\lambda_n = 0$ or π, thus $e^{j\lambda_n} = e^{-j\lambda_n}$. So, the amplitude for code word $\hat{c}$ is

$$
\begin{aligned}
|S_{\hat{c}}(t)| &= \ \left| \sum_{n=0}^{N-1} e^{j\frac{2\pi n}{N}\frac{t}{T_d}} e^{j\lambda_n} \right| \\
&= \ |S_c(t)| \tag{2.14}
\end{aligned}
$$

Thus, the amplitude is the same for c and $\hat{c}$, and the PAPR is also the same for c and $\hat{c}$.

4. The ideal PAPR

If the power spectrum $S(f)$ of the signal $S(t)$ in Equation (2.1) is a constant, then the peak power of the signal $S(t)$ is the same as the average power of the signal $S(t)$. The ideal PAPR is reached, that is, $PAPR = 1$.

2.4 High Power Amplifier

The nonlinear High Power Amplifier(HPA) can be modeled as a memoryless device [15]. The complex baseband input signal of the HPA can be expressed by the magnitude $r(t)$ and phase $\phi(t)$

$$x(t) = r(t)e^{-j\phi(t)} \tag{2.15}$$

The nonlinear distorted signal at the output of the HPA is

$$y(t) = R(t)e^{-j\Phi(t)} \tag{2.16}$$

The AM/AM conversion (amplitude nonlinearity) $R(t) = f(r(t))$ describes the nonlinear function between the input and output amplitude. The AM/PM conversion(phase nonlinearity) $\Phi(t) = g(r(t))$ produces an additional phase modulation.

The following are two types of HPA: Travelling Wave Tube Amplifier(TWTA) and Solid State Power Amplifier(SSPA), which are commonly used in the literature.

2.4.1 Travelling Wave Tube Amplifier(TWTA)

The AM/AM conversion function of the TWTA [15] is

$$R(t) = \frac{2r(t)}{1 + r^2(t)} \tag{2.17}$$

The AM/PM conversion function is

$$\Phi(t) = \phi(t) + \frac{\pi}{3}\frac{r^2(t)}{1 + r^2(t)} \tag{2.18}$$

Here, the input and the output amplitude are normalized by the saturation amplitude A_{clip}. The AM/AM conversion and the AM/PM conversion of the TWTA are shown in Figure 2.4.
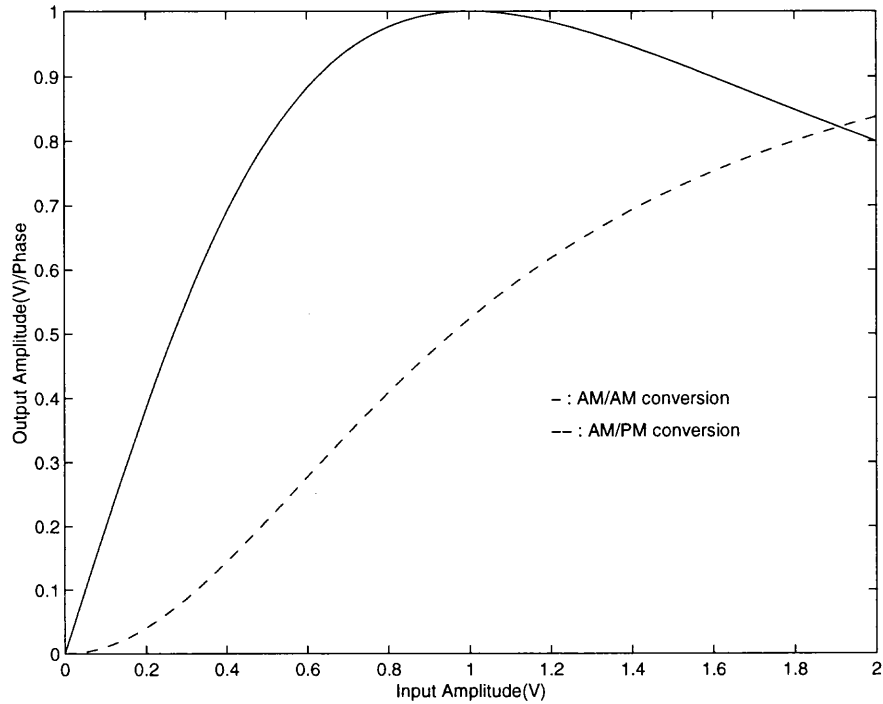
Figure 2.4 Diagram of Normalized AM/AM Conversion for Travelling Wave Tube Amplifier

2.4.2 Solid State Power Amplifier(SSPA)

The AM/AM conversion function of the SSPA [15] is

$$R(t) = \frac{r(t)}{\left(1 + (r(t))^{10}\right)^{\frac{1}{10}}} \tag{2.19}$$

The AM/PM conversion function is

$$\Phi(t) = \phi(t) \tag{2.20}$$

The Amplitude/Amplitude(AM/AM) conversion of the SSPA is shown in Figure 2.5. Here, the SSPA produces no phase distortion.
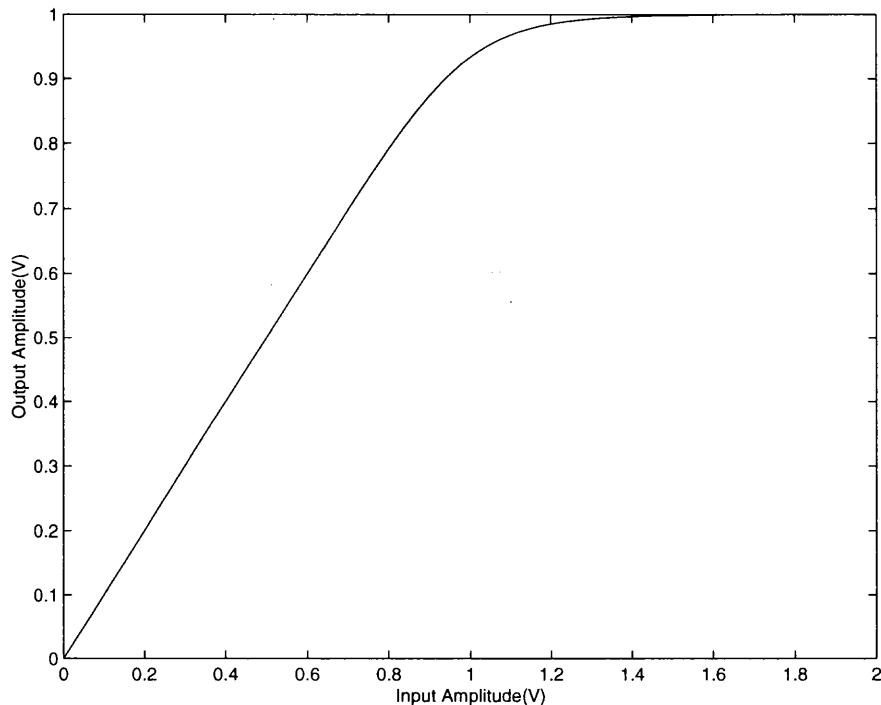
Figure 2.5 Diagram of Normalized AM/AM Conversion for Solid State Power Amplifier

2.4.3 Input and Output Back-offs

The non-linear distortions of HPA depend strongly on the input back-off(IBO) and the output back-off(OBO) [15], which are defined as

$$IBO = \frac{P_{sat}}{P_{in}} \tag{2.21}$$

$$OBO = \frac{P_{sat}}{P_{out}} \tag{2.22}$$

where $P_{sat} = A_{clip}^2$ is the saturation power of the HPA, $P_{in} = E(|x(t)|^2)$ is the mean power of the input signal $x(t)$ and $P_{out} = E(|y(t)|^2)$ is the mean power of the output signal $y(t)$ of the HPA.

2.5 Predistortion Techniques

To make better use of the available HPA power, some compensation techniques can be used at the transmitter side.

Let $z(t) = |z(t)|e^{-j\psi(t)}$ be the signal that has to be amplified and $y(t) = R(t)e^{-j\Phi(t)}$ the amplified signal. Since the HPA is non-linear device, the resulting output will be distorted. To limit this distortion, a device with output signal $x(t) = r(t)e^{-j\phi(t)}$ can be inserted in baseband before the HPA in order that the HPA output $y(t)$ is as close as possible to the original signal $z(t)$. The procedure is shown is Figure 2.6.

```
z(t)                              x(t)                    y(t)
  ──────▶│  Predistortion  │──────────▶│      HPA      │──────▶
```
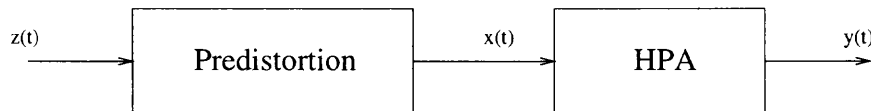
Figure 2.6 Diagram of HPA with Predistortion

2.5.1 TWTA

In order to cancel the non-linearity of TWTA, the inversion of the TWTA equation (2.17) and equation (2.18) lead to the following equations:

$$r(t) = \begin{cases} \frac{1}{|z(t)|}[1 - \sqrt{1 - |z(t)|^2}] & \text{if } |z(t)| < 1 \\ 1 & \text{if } |z(t)| \geq 1 \end{cases} \qquad (2.23)$$

and

$$\phi(t) = \begin{cases} \psi(t) - \frac{\frac{\pi}{3}r(t)^2}{1+r(t)^2} & \text{if } |z(t)| < 1 \\ \psi(t) - \frac{\pi}{6} & \text{if } |z(t)| \geq 1 \end{cases} \qquad (2.24)$$

2.5.2 SSPA

In order to cancel the non-linearity of TWTA, the inversion of the TWTA equation (2.19) and equation (2.20) lead to the following equations:

$$r(t) = \frac{|z(t)|}{(1 - |z(t)|^{10})^{\frac{1}{10}}} \qquad (2.25)$$

and

$$\phi(t) = \psi(t) \qquad (2.26)$$

2.5.3 The Compensated HPA

From Figure 2.6, if $r(t)$ and $\phi(t)$ in Equation (2.17) and (2.18) are substituted by Equation (2.23) and (2.24), we can get

$$R(t) = \begin{cases} |z(t)| & \text{if } |z(t)| < 1 \\ 1 & \text{if } |z(t)| \geq 1 \end{cases} \tag{2.27}$$

and

$$\Phi(t) = \psi(t) \tag{2.28}$$

We can get the same results with SSPA. Considering the saturation amplitude of HPA is normalized by A_{clip}, so the compensated HPA is presented as

$$y(t) = \begin{cases} z(t) & \text{if } |z(t)| < A_{clip} \\ A_{clip}\frac{z(t)}{|z(t)|} & \text{if } |z(t)| \geq A_{clip} \end{cases} \tag{2.29}$$

where $z(t)$ is the signal that has to be amplified and $y(t)$ is the amplified signal. A_{clip} is the saturation amplitude of HPA. When $|z(t)|$ is larger than A_{clip}, the signal is clipped, so A_{clip} is also called the clipping level of HPA. A compensated HPA is shown in Figure 2.7.

2.6   Clipping Effects

After a compensated High Power Amplifier, the signal is clipped. Here, the power of the clipping noise and the probability that the signal amplitude is greater than the clipping level A_{clip} are discussed [18]. If the total power of the unclipped and undistorted OFDM signal is $2\sigma^2$, the input back-off(IBO) can be represented as

$$IBO = 10\log_{10}\frac{A_{clip}^2}{2\sigma^2} = 10\log_{10}\frac{\mu^2}{2} \tag{2.30}$$

Where $\mu = \frac{A_{clip}}{\sigma}$.

Following the approximation approach in [18], the real and imaginary parts of $N-$point IFFT output samples have mutually independent Gaussian probability distribution function(pdf) with zero mean and variance σ^2. Therefore the amplitude
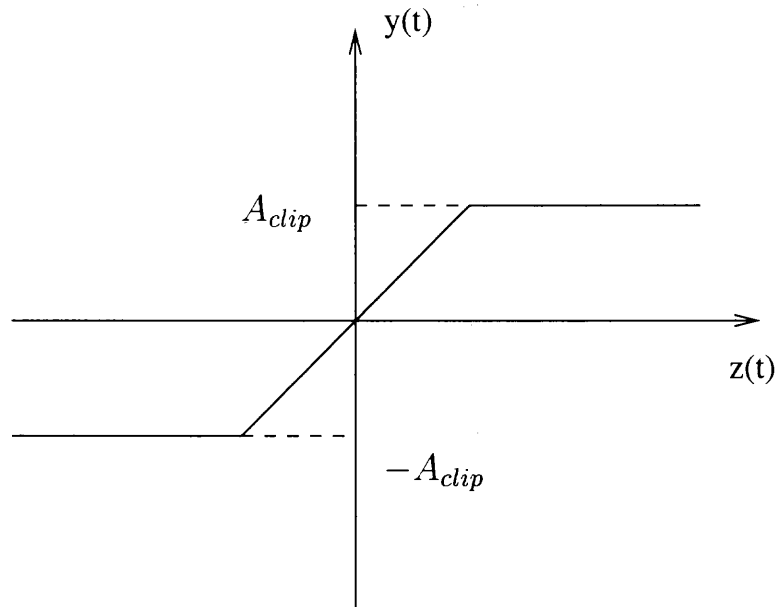
Figure 2.7 Block Diagram of a compensated HPA

of the OFDM signal x has a Rayleigh distribution and its phase is uniformly distributed. that is

$$f(x) = \frac{x}{\sigma^2} e^{-\frac{x^2}{2\sigma^2}} \tag{2.31}$$

Because the maximum amplitude of the OFDM signal is limited to A_{clip}, the power of the clipped portion is

$$
\begin{aligned}
P_{clip} &= \int_{A_{clip}}^{\infty} x^2 f(x) dx \\
&= e^{-\frac{A_{clip}^2}{2\sigma^2}} (2\sigma^2 + A_{clip}^2) \\
&= e^{-\frac{\mu^2}{2}} (2\sigma^2 + A_{clip}^2)
\end{aligned}
\tag{2.32}
$$

Thus, the signal-to-clipped-noise power ratio can be expressed as

$$
\begin{aligned}
(SNR_{clip})_{dB} &= \frac{2\sigma^2}{P_{clip}} \\
&= -10 \log_{10} \left(e^{-\frac{\mu^2}{2}} (1 + \frac{\mu^2}{2}) \right)
\end{aligned}
\tag{2.33}
$$

The relation between IBO and the signal-to-clipped-noise ratio is expressed in Figure 2.8. In order to get the output power of the HPA, first calculate the probability of
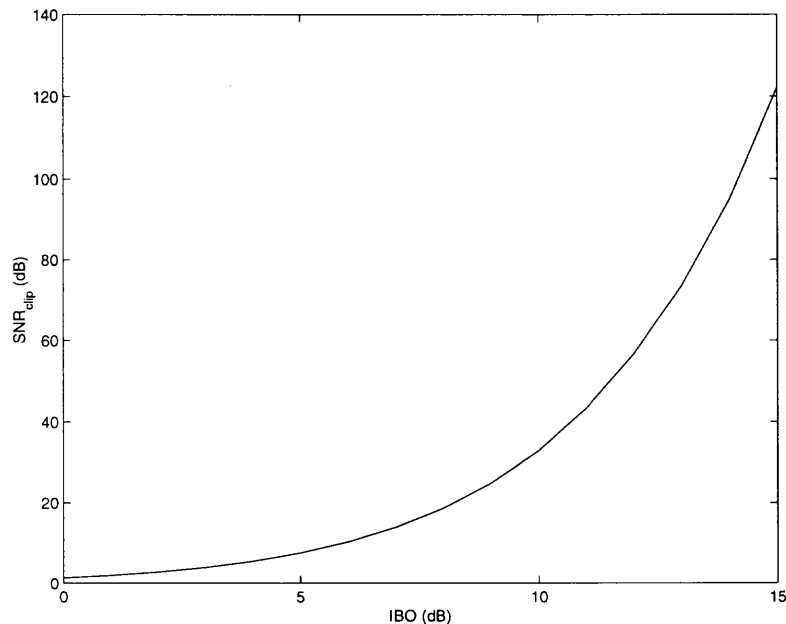
Figure 2.8 Diagram of Signal-to-Clipping Noise Ratio Versus IBO

the amplitude of the signal x greater than A_{clip}. That is

$$
\begin{aligned}
p(x \geq A_{clip}) &= \int_{A_{clip}}^{\infty} f(x)dx \\
&= e^{-\frac{\mu^2}{2}}
\end{aligned}
\tag{2.34}
$$

The output power of the HPA consists of two parts: one is that of the original signal which amplitude is under A_{clip}, $(2\sigma^2 - P_{clip})$, the other is that of the clipping level A_{clip}. So the total power output, P_{tot} after clipping is

$$
P_{tot} = 2\sigma^2 - P_{clip} + A_{clip}^2 \cdot p(x \geq A_{clip})
\tag{2.35}
$$

Substituting for P_{clip} from Equation (2.32) and using Equation (2.34), we get

$$
P_{tot} = 2\sigma^2(1 - e^{-\frac{\mu^2}{2}})
\tag{2.36}
$$

The Output-backoff (OBO) is

$$
\begin{aligned}
OBO &= 10log_{10}\frac{A_{clip}^2}{P_{tot}} \\
&= -10log_{10}(\frac{2}{\mu^2}(1 - e^{-\frac{\mu^2}{2}}))
\end{aligned}
\tag{2.37}
$$
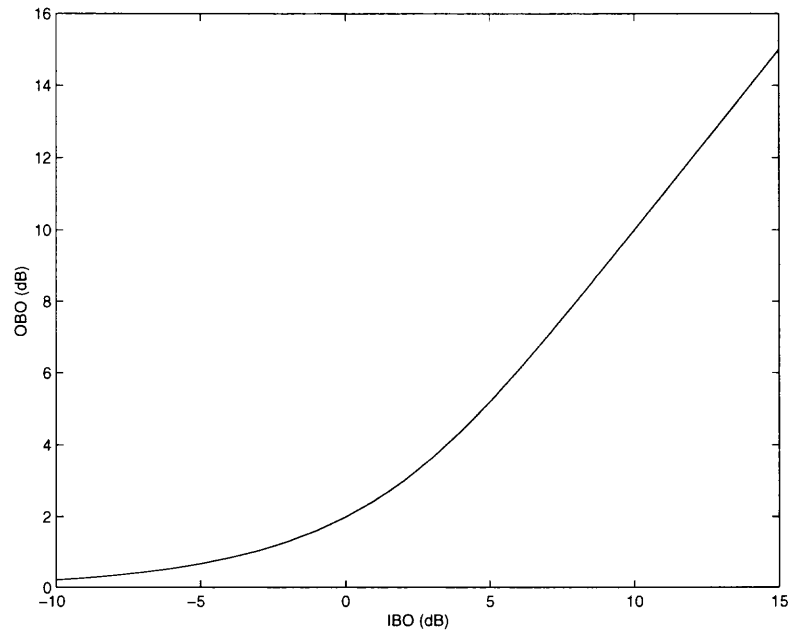
Figure 2.9 OBO Versus IBO

Using Equation (2.37) and Equation (2.30), we get the relation between OBO and IBO

$$OBO = IBO - 10\log_{10}\left(1 - e^{-\frac{\mu^2}{2}}\right) \tag{2.38}$$

Which is depicted in Figure 2.9.

The clipping effect on the Signal to Noise Ratio(SNR) versus Bit Error Rate(BER) in OFDM system is illustrated in Figure 2.10, where the clipping level A_{clip}^2 is normalized by the noise power σ^2. The length of the code word is $N = 8$. The clipping level is the saturation power of a compensated HPA, that is, A_{clip}^2. If A_{clip}^2 is greater than $N^2 = 64$, there is no clipping effect actually, which is shown by the curve without clipping. With lower clipping level in a compensated HPA, the transmitted signal will suffer higher distortion, so BER is higher. In order to decrease BER with the same SNR for a compensated HPA with lower clipping level, some coding techniques are discussed in the next section.
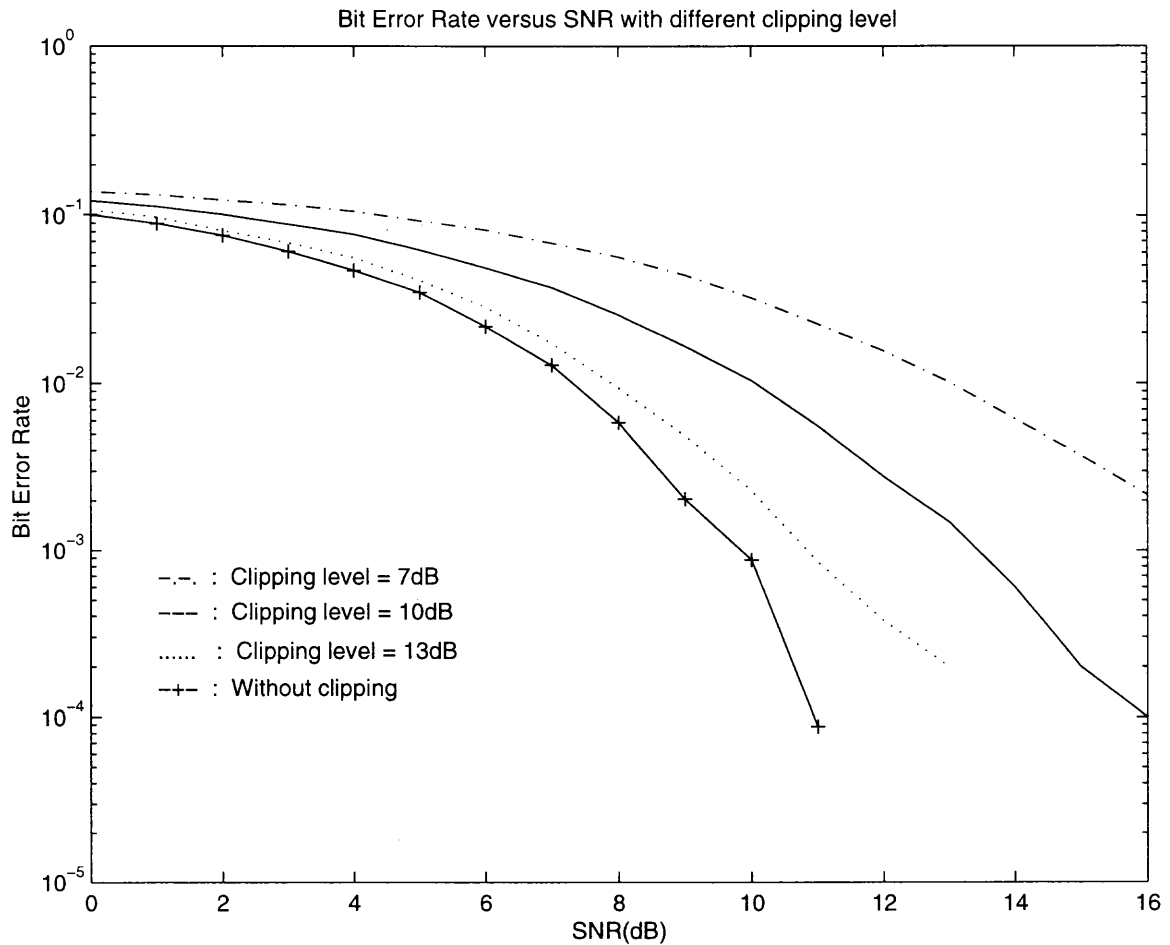
Figure 2.10 Bit Error Rate Versus SNR with Different Clipping Level(N=8)

2.7   Coding Techniques

In order to minimize PAPR of the OFDM signal, coding scheme is commonly used. In this section, first, several coding techniques are discussed. Then, a new coding scheme is proposed and compared with other schemes.

2.7.1   Linear Block Coding

A block code consists of a fixed-length vector is called code word [19, 20]. The length N of the a code word is the number of the elements in the vector. The elements of a code word are selected from an alphabet of q elements. Considering symbols with BPSK modulation, the alphabet consists of two elements, $\{0, 1\}$. Because the input

block code word is random, there are 2^N possible code words. Different code word have different PAPR for the OFDM signal. These code words with lower PAPR are the ones that are preferred for transmission. Coding schemes are used to eliminate the codewords with higher PAPR.

From 2^N possible code words in a binary block code of length N, only $M = 2^K$ code words $(K < N)$ are selected to form a code. That is, a block of K information bits is mapped into a code word of length N. The resultant block code is called a (N, K) code. The ratio $K/N = R$ is defined as the rate of the code. K bits are the information bits and $N - K$ bits are the redundancy bits. The tradeoff for the reduction of PAPR is the decrease of the net bit rate.

A simple odd parity code was proposed by Dr. A. E. Jones [4]. From Equation (2.1) the output of the transmitter is

$$S(t) = \sum_{n=1}^{N} d_n(t) e^{j(2\pi f_n + \beta_n)} \tag{2.39}$$

For the number of carriers N is 4, the envelope power of the OFDM for all possible code words is given in Figure 2.11. Using one bit Odd Parity Coding technique, the three-bit information code word can be converted into four-bit code word. Obviously only the code words with lower PAPR should be chosen for transmission. Table 2.1 gives the look-up table for this one odd parity method.

Using Odd Parity coding, the resultant envelope power for all possible information code words is plotted in Figure 2.12.

The PAPR for all possible four-bit code words is

$$PAPR_{4c} = 10log(\frac{16}{4}) = 6.02dB \tag{2.40}$$

After the coding, the PAPR for all possible three-bit code words is

$$PAPR_{4cad} = 10log(\frac{7.07}{4}) = 2.47dB \tag{2.41}$$
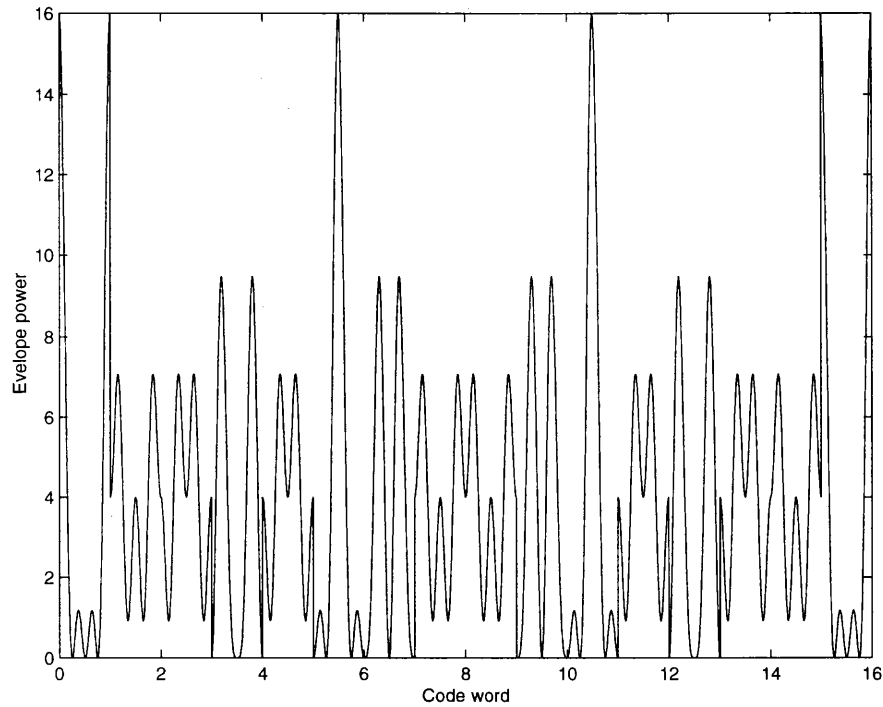
Figure 2.11 Envelope Power for All Possible Code Words (N=4)

There is a $3.55dB$ PAPR reduction for this $3/4$ rate code, but the expense is an increase in bandwidth for the same net data rate and a reduction in the energy per transmitted bit $\frac{E_b}{N_0}$ for the same transmit power.

Block coding scheme is simple for application, but not so effective in reducing PAPR when the number of carriers N increases. This can be shown in Table 2.2.

Information	Code
000	0001
001	0010
010	0100
011	0111
100	1000
101	1011
110	1101
111	1110

Table 2.1 Odd Parity Code
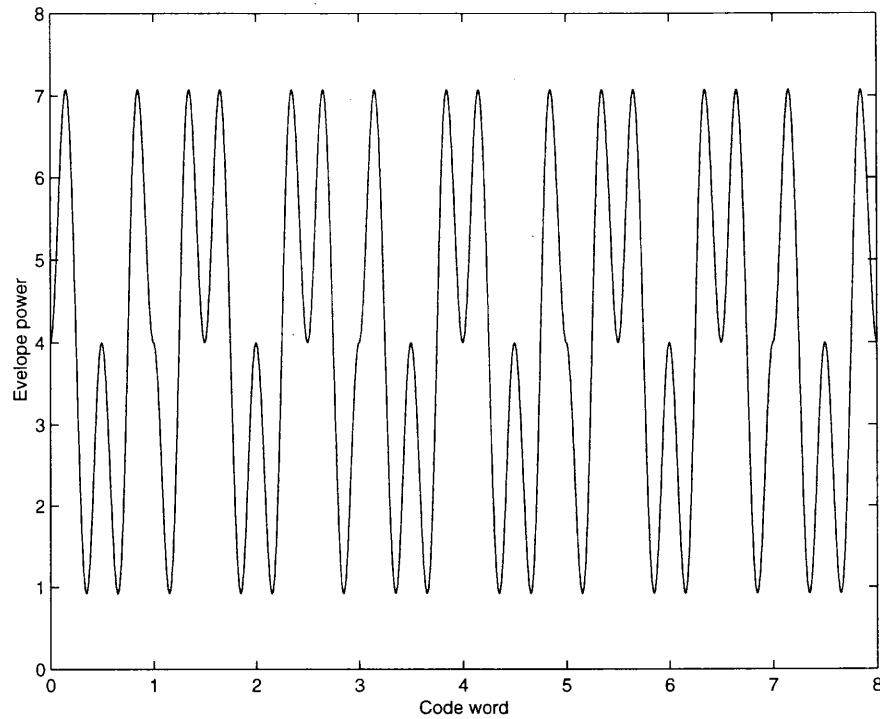
Figure 2.12 Envelope Power for All Possible Code Words (K=3,N=4)

N	$PAPR_m(dB)$	$PAPR_b(dB)$	REDUCTION
4	6.02	2.47	3.55
8	9.03	6.53	2.50
12	10.79	8.96	1.83
16	12.04	10.88	1.16
32	15.05	14.49	0.56

Table 2.2 PAPR Reduction with Block Coding

2.7.2 Cyclic Coding Scheme (Subblock Coding Scheme)

In this section, a difficult coding scheme is discussed. It was proposed by D.Wulich [21]. Though it is called cyclic coding scheme, but actually it is just an improvement to block coding scheme. Hence it is also called subblock coding scheme [22].

OFDM as a Multi-carrier modulation, can be represented (not in baseband equivalent) as:

$$s'(t) = \sum_{n=1}^{N} \cos[(w_0 + n\Delta w)t + \phi_n] \qquad 0 < t < T \qquad (2.42)$$

where $\Delta w = \frac{2\pi}{T}$ and ϕ_n can be 0 or π for BPSK. The PAPR is

$$PAPR = 10 \log_{10} \frac{max(|s'(t)|^2)|_{0<t<T}}{N} \qquad (2.43)$$

First, $s'(t)$ is rewritten as

$$
\begin{aligned}
s'(t) &= \sum_{n=1,odd}^{N-1} \{\cos[(w_0 + n\Delta w)t + \phi_n] + \cos[(w_0 + (n+1)\Delta w)t + \phi_{n+1}]\} \\
&= 2 \sum_{n=1,odd}^{N-1} \cos(\frac{\Delta wt}{2} + \frac{\phi_{n+1} - \phi_n}{2}) \times \cos[(w_0 + n\Delta w + \frac{\Delta w}{2})t + \frac{\phi_{n+1} + \phi_n}{2}]
\end{aligned}
$$

$$(2.44)$$

It is easy to prove that

$$|s'(t)| \le 2 \sum_{n=1,odd}^{N-1} |\cos(\frac{\Delta wt}{2} + \alpha_n)| \qquad (2.45)$$

where $\alpha_n = \frac{\phi_{n+1} - \phi_n}{2}$, which can be $0, -\frac{\pi}{2}$ or $\frac{\pi}{2}$.

Choosing $N = 4L$, where L is any positive integer, the equation 2.45 can be represented as

$$|s'(t)| \le 2 \sum_{l=1}^{4L-3} |\cos(\frac{\Delta wt}{2} + \alpha_l)| + |\cos(\frac{\Delta wt}{2} + \alpha_{l+2})| \qquad (2.46)$$

Where $l = 1, 5, \cdots, 4L - 3$, note that the number of terms is $L = N/4$.

Now if

$$|\alpha_{l+2} - \alpha_l| = \frac{\pi}{2} \qquad l = 1, 5, \cdots, 4L - 3 \qquad (2.47)$$

Then Equation (2.46) can be rewritten as

$$|s'(t)| \le 2 \sum_{l=1}^{4L-3} |\cos(\frac{\Delta wt}{2} + \alpha_l)| + |\sin(\frac{\Delta wt}{2} + \alpha_l)| \qquad (2.48)$$

From the following equation

$$|\cos(\theta)| + |\sin(\theta)| \le \sqrt{2} \qquad (2.49)$$

One can conclude that

$$|s'(t)| \le 2\sqrt{2}L \qquad (2.50)$$

$\tilde{\phi}_l$	ϕ_{l+1}	ϕ_{l+2}	ϕ_{l+3}
0	0	0	π
π	0	0	0
0	π	0	0
π	π	0	π
0	0	π	0
π	0	π	π
0	π	π	π
π	π	π	0

Table 2.3 Cyclic Coding

That is

$$|s'(t)| \leq \frac{N}{\sqrt{2}} \tag{2.51}$$

Thus, the peak to average power ratio of the signal $s'(t)$ is

$$PAPR = \frac{|s'(t)|^2}{N} \leq \frac{N}{2} \tag{2.52}$$

which means the maximum value of the PAPR is reduced by $3dB$ compared with the uncoded case.

From Equation (2.47), The condition can be represented as

$$\left|\frac{\phi_{l+3} - \phi_{l+2}}{2} - \frac{\phi_{l+1} - \phi_l}{2}\right| = \frac{\pi}{2} \qquad l = 1, 5, \cdots, N-3 \tag{2.53}$$

Considering a specific condition

$$\phi_{l+3} = -\phi_l + \phi_{l+1} + \phi_{l+2} + \pi \ (mod \ 2\pi) \qquad l = 1, 5, \cdots, N-3 \tag{2.54}$$

Where ϕ_l is 0 or π for BPSK modulation. If the algorithm of Equation (2.54) is used, then Equation (2.53) is satisfied. This scheme can be shown in Table 2.3. If changing π with 1, then Table 2.3 is the same as Table 2.1.

Actually, cyclic coding scheme can be described as: first separate a code word with length $3L$ into L code words with a length 3, then apply the block coding scheme to these L code words respectively. This is why the cyclic coding scheme is also called the subblock coding scheme. The resultant code word has a length $4L$. The code

rate is 3/4.

The simulation of PAPR reduction with this cyclic coding method is shown in the Table 2.4. The second column is the PAPR without coding, the third column is the PAPR with cyclic coding and the fourth column is the PAPR reduction. It can be seen this scheme is much better than the block coding scheme compared with Table 2.2.

N	$PAPR_m(dB)$	$PAPR_c(dB)$	REDUCTION
4	6.02	2.47	3.55
8	9.03	5.36	3.67
12	10.78	7.05	3.73
16	12.04	8.30	3.74
32	15.05	10.20	4.85

Table 2.4 PAPR with Cyclic Coding

2.7.3 A Novel Subblock Coding Scheme with Bit Position Control

Using the block coding and the subblock coding techniques can reduce the PAPR in OFDM system. However, for the block coding schemes, when the length N of the code word becomes larger, the PAPR reduction decreases rapidly.

In order to further reduce PAPR when the carrier number N is large, some modifications are suggested for block coding method. we will also use the assumption $N = 4L$, where $L = 1, 2, \ldots, \infty$.

1. First using a Serial-to-Parallel converter, the input data is converted into a code word which is expressed

$$\mathbf{d} = [d_1(1), d_1(2), d_1(3), \ldots, d_L(1), d_L(2), d_L(3)] \qquad (2.55)$$

The length of the code word $\mathbf{d}$ is $3L$. Separating the code word $\mathbf{d}$ into some subblocks and then use odd parity coding method to get the redundancy bit. This procedure is shown in Figure 2.13. The resultant code word $\mathbf{c}$ can be

expressed as

$$\mathbf{c} = [c(1), c(2), \ldots, c(N)]$$

$$= [d_1(1), d_1(2), d_1(3), P_1(1), \ldots, d_L(1), d_L(2), d_L(3), P_L(1)] \quad (2.56)$$

where $P_n(1)$ is an odd parity and the length of the resultant code word c is $4L$.

$$P_n(1) = d_n(1) \oplus d_n(2) \oplus d_n(3) \oplus 1 \quad (2.57)$$
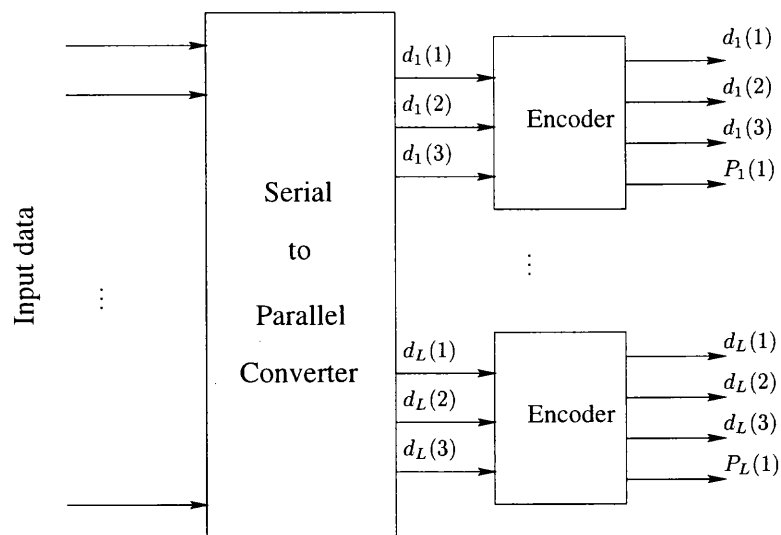
Figure 2.13 Block Diagram of A Subblock Coding Encoder

2. In block coding scheme, the position of the odd parity bit $P_n(1)$ is fixed at the end of each subblock code word, so PAPR reduction is fixed for each code word. With the new block scheme we consider all possible position of $P_n(1)$ in each block $d_n(1), d_n(2), d_n(3)$. That is, the resultant block code word can be $d_n(1), d_n(2), d_n(3), P_n(1)$ or $d_n(1), d_n(2), P_n(1), d_n(3)$ or $d_n(1), P_n(1), d_n(2), d_n(3)$ or $P_n(1), d_n(1), d_n(2), d_n(3)$. Then these different subblocks are combined to form a code word for transmission.

3. Before transmission, a feedback scheme is used to choose the code word with the lowest PAPR for transmission. PAPR of the code word c is found in PAPR

calculator. Bit position control block is used to change the position of $P_n(1)$ in the block $d_n(1), d_n(2), d_n(3)$. As a result, different code words are produced in the bit position encoder. Different PAPR for different code words are compared in the code word selector, then the code word with the lowest PAPR is recorded and chosen for transmission. The system need a lot of comparison. It need compare totally $4^{N/4}$ times to get the desired code word. Therefore, when N is a large number, we need to find some method to reduce the system complexity. The position information of $P_n(1)$ is also transmitted as side information so the receiver can decode the information. This procedure is illustrated in Figure 2.14.
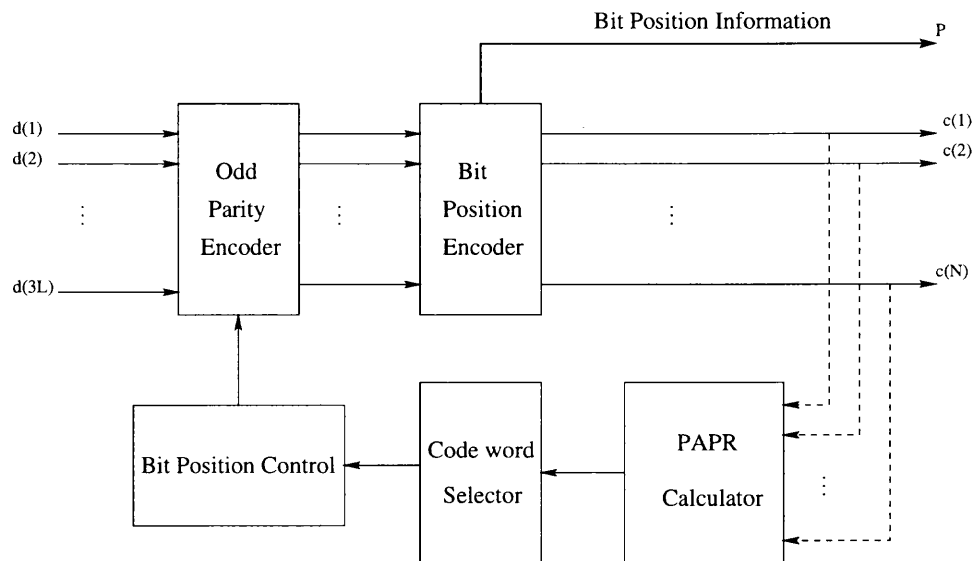
Figure 2.14 Block Diagram of A Novel Subblock Coding Scheme with Bit Position Control

The simulation of PAPR reduction with this novel block coding scheme with bit position control is shown in the Table 2.5. The second column is the PAPR without coding, the third column is the PAPR with this new coding scheme and the fourth column is the PAPR reduction. It can be seen this scheme is much better than the cyclic(subblock) coding scheme compared with Table 2.4.

N	$PAPR_m(dB)$	$PAPR_n(dB)$	REDUCTION
4	6.02	2.47	3.55
8	9.03	3.84	5.19
12	10.78	4.77	6.01
16	12.04	6.02	6.02
32	15.05	6.73	8.32

Table 2.5 PAPR with the Novel Coding

2.8 Simulation Results

In this section, the simulation results of an OFDM system with PAPR reduction is discussed. Here assuming the subcarrier number is $N = 8$, and the length of the input code word is $L = 6$. The code rate is 3/4 without considering the side information.

2.8.1 PAPR Reduction Using A Novel Coding Scheme with A Specific Code Word

Here, an example is given to show the PAPR reduction using this novel block coding scheme is better than subblock coding scheme. Because the code words produced with this new coding scheme include the code word produced with the subblock coding scheme, this new coding scheme has at least the same PAPR reduction as the subblock coding scheme. In fact, this new coding scheme is much better than the subblock coding scheme. The payoff is the intensive calculation used for choosing the lowest PAPR for transmission.

The code word A without coding scheme is 000000. The code word B with subblock coding scheme is 00010001. The code word C with this novel coding scheme is 00010010. The instantaneous power of code word A,B and C in one time duration is shown in Figure 2.15, Figure 2.16 and Figure 2.17. From these figures we can see that be PAPR is lowest for the novel block coding scheme with position bit control.
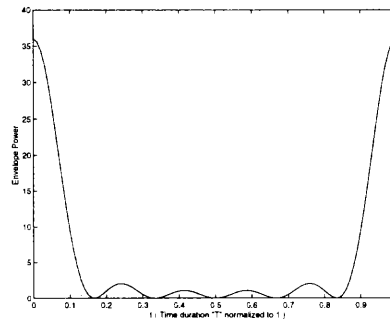
Figure 2.15 Diagram of the Envelope Power of the Code Word 000000
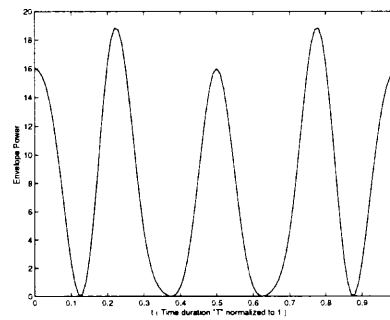
Figure 2.16 Diagram of the Envelope Power of the Code Word 00010001
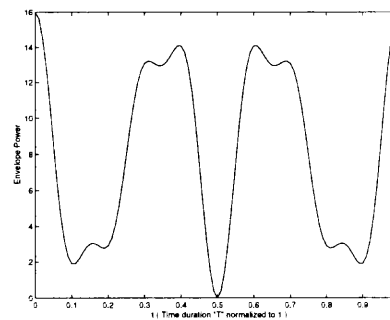
Figure 2.17 Diagram of the Envelope Power of the Code Word 00010010

2.8.2 Peak Power Effect

The PAPR can be evaluated by the peak power of the transmitted signal, because the average power is a constant number N. The effect on the peak power with different coding schemes is plotted in Figure 2.18. If we generate random code words, then we will get different peak power x for different code words. x-axis represents a fixed power value X and y-axis represents the probability when the peak power x is larger than X. Derived from this figure, the signal peak power is 64 without coding scheme, which can be calculated theoretically. The theoretical peak power is $N^2 = 64(N = 8)$. Using subblock coding scheme, the peak power is reduced to 27.7. Using block coding with bit position control scheme, the peak power is reduced to 19.4. So it can be concluded that this new novel scheme can reduce the PAPR significantly.
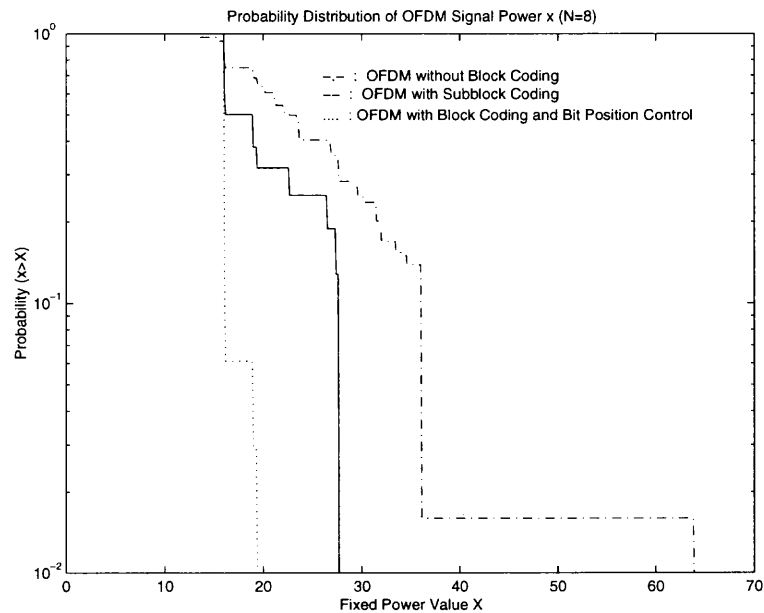
Figure 2.18 Diagram of Probability Distribution Function of OFDM Signal Amplitude x
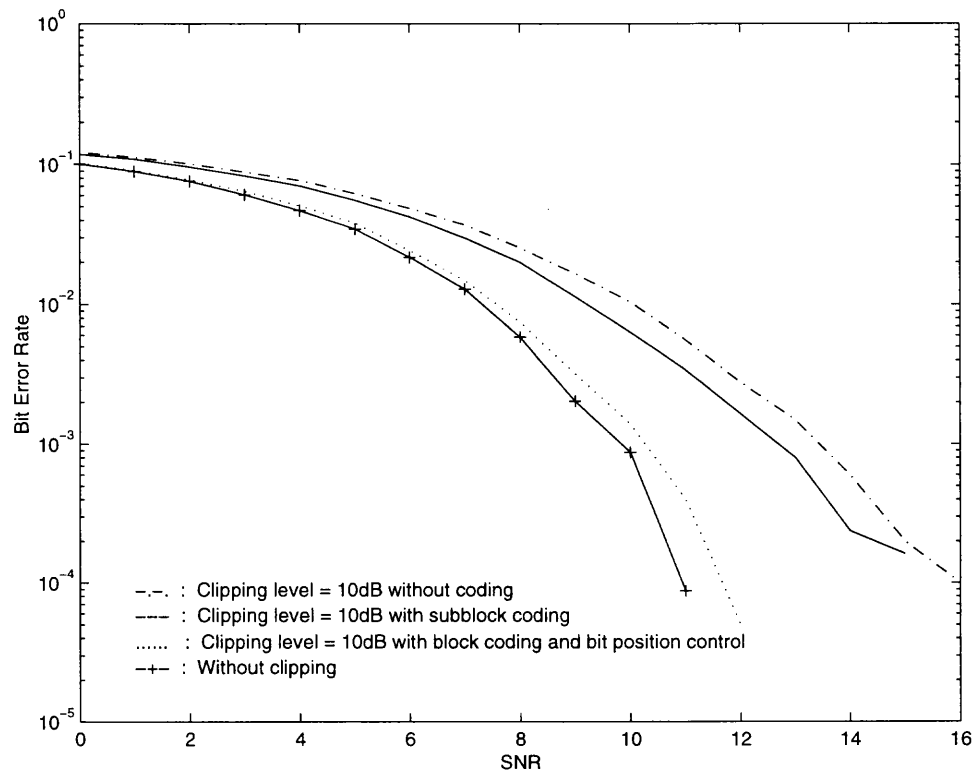
Figure 2.19 Block Diagram of BER Versus SNR Using A Novel Block Coding Scheme with Bit Position Control

2.8.3 Bit Error Rate Improvement

The BER of the OFDM system is plotted in Figure 2.19. The clipping level is 10dB for a compensated HPA. The clipping level is the saturation power of HPA. The length of the code word for IFFT modulation is $N = 8$. It can be seen that if we only use subblock coding for PAPR reduction, the PAPR is reduced somewhat, but BER for the same SNR only improve slightly. When bit position control is added in the subblock coding, BER improves substantially, BER versus SNR curve in this case is quite close to the theoretical curve.

CHAPTER 3

COMMUNICATION CHANNEL

The signal at the output of the transmitter will go through a propagation channel before reaching the receiver. The original transmitted signal will suffer different frequency and amplitude variation in different channel models. Here three channel models are discussed.

3.1   Characterization of Multipath Channel

Because the natural and man-made objects are in the immediate vicinity of the mobile stations, no direct line-of-sight(LOS) path exists between the base station(BS) and mobile station(MS) antenna. As a consequence of reflections, scattering and diffraction, the received signal has different directions and different delays. This property is called multipath propagation [23].

Consider the transmission of the band-pass signal is

$$s(t) = u(t) \cos 2\pi f_c t \tag{3.1}$$

where $u(t)$ is the real low-pass signal , f_c is the carrier frequency. Assuming that there are multiple propagation paths, the received bandpass signal can be expressed in the form

$$x(t) = \sum_{n=1}^{N} \alpha_n(t) s(t - \tau_n(t)) \tag{3.2}$$

where $\alpha_n(t)$ and $\tau_n(t)$ are the amplitude attenuation factor and the time delay of the nth path for the received signal respectively.

Substituting for $s(t)$ from Equation 3.1 into Equation 3.2 , the result is

$$
\begin{aligned}
x(t) &= \sum_{n=1}^{N} \alpha_n(t) u(t - \tau_n(t)) \cos 2\pi f_c(t - \tau_n(t)) \} \\
&= \sum_{n=1}^{N} \alpha_n(t) Re\{u(t - \tau_n(t)) e^{j2\pi f_c(t - \tau_n(t))} \}
\end{aligned}
$$

$$= Re\{[\sum_{n=1}^{N} \alpha_n(t)e^{-j\pi f_c\tau_n(t)}u(t-\tau_n(t))]e^{j2\pi f_c t}\} \qquad (3.3)$$

Thus, the equivalent lowpass received signal is

$$r(t) = \sum_{n=1}^{N} \alpha_n(t)e^{-j\pi f_c\tau_n(t)}u(t-\tau_n(t))$$

$$= \sum_{n=1}^{N} \alpha_n(t)e^{-j\pi f_c\tau_n(t)}\delta(\tau-\tau_n(t)) * u(t-\tau) \qquad (3.4)$$

From Equation 3.4 , the channel can be modeled by a time-variant linear filter having the complex low-pass impulse response

$$c(\tau,t) = \sum_{n=1}^{N} \alpha_n(t)e^{-j\pi f_c\tau_n(t)}\delta(\tau-\tau_n(t)) \qquad (3.5)$$

where $c(\tau;t)$ is the channel response at time t to an impulse applied at time $t-\tau$, and $\delta(\cdot)$ is the dirac delta function.

Considering the addition of white Gaussian noise $n(t)$, the received signal is

$$r(t) = c(\tau,t) * u(t-\tau) + n(t) \qquad (3.6)$$

3.1.1 Gaussian Non-fading Channel

If the channel is assumed to corrupt the transmitted signal by only the addition of white Gaussian noise, that is, there is only LOS component in the receiver, the channel is called Additive White Gaussian Channel(AWGN) channel.

The probability density function of the Gaussian variable x is

$$f(x) = \frac{1}{\sqrt{2\pi}\sigma}e^{-\frac{(x-\mu)^2}{2\sigma^2}} \qquad (3.7)$$

where μ is the mean and σ^2 is the variance of the random variable x.

3.1.2 Rayleigh Fading Channel

When considering the transmission of an unmodulated carrier and the composite received signal consists of a large number of path components, the received complex low-pass signal $r(t) = r_I(t) + jr_Q(t)$ can be modeled using central limit theorem as a

complex Gaussian random process. This means the channel impulse response $c(\tau; t)$ is a complex Gaussian random process in the variable t.

In the absence of a LOS, $r_I(t)$ and $r_Q(t)$ have zero-mean. The envelope $|c(\tau; t)|$ has a Rayleigh distribution at any time t and th phase of $c(\tau; t)$ has a uniform distribution in the interval$(0, 2\pi)$. The channel is called to be a Rayleigh fading channel.

The probability density function of the Rayleigh fading variable $r(t)$ is

$$f(r) = \frac{r}{\sigma^2} e^{-\frac{r^2}{2\sigma^2}} \tag{3.8}$$

where σ^2 is the variance of $r_I(t)$ and $r_Q(t)$. The kth moment of r is

$$E(r^k) = (2\sigma^2)^{\frac{k}{2}} \Gamma(1 + \frac{1}{2}k) \tag{3.9}$$

Where Γ is the Gamma function. $\Gamma(\frac{1}{2}) = \sqrt{\pi}$. $\Gamma(n + \frac{1}{2}) = \frac{1 \cdot 3 \cdot 5 \cdots (2n-1)}{2^n} \sqrt{\pi}$ and $\Gamma(n) = (n - 1)!$ for n is an integer, $n > 0$.

Thus, the mean μ and the variance σ_r^2 are

$$\mu = E(r) = \sqrt{\frac{\pi}{2}} \sigma \tag{3.10}$$

$$\begin{aligned}
\sigma_r^2 &= E[(r - \mu)^2] \\
&= E[r^2] - \mu^2 \\
&= 2\sigma^2 \Gamma(2) - \frac{\pi}{2} \sigma^2 \\
&= (2 - \frac{\pi}{2}) \sigma^2
\end{aligned} \tag{3.11}$$

3.1.3 Ricean Fading Channel

For a multipath fading channel containing a LOS component, the received signal will include both a LOS component and other multipath components. The real and image part of the received signal, $r_I(t)$ and $r_Q(t)$ have non-zero mean. The envelope $|c(\tau; t)|$ has a Ricean distribution at any time t, and The channel is called to be a Ricean fading channel. Ricean fading is often observed in microcellular applications.

The probability density function of the Ricean fading variable $r(t)$ is

$$f(r) = \frac{r}{\sigma^2} e^{-\frac{r^2+s^2}{2\sigma^2}} I_0(\frac{rs}{\sigma^2}) \qquad (3.12)$$

where s^2 is the non-centrality parameter, which represents the power of the LOS component. The parameter σ^2 is the power of the scattered components. $I_0(\cdot)$ is the zero order Bessel function. Here, a Rice factor K is defined as

$$K = \frac{s^2}{2\sigma^2} \qquad (3.13)$$

which is ratio of the power of the LOS component to the power of the scattered component. When $K = 0$, that means there is no LOS component, Ricean fading channel will turn into Rayleigh fading channel. When $K = \infty$, that means there is only the LOS component and no multipath components, Ricean fading channel will turn into Gaussian non-fading channel.

The mean and variance of the Ricean fading variable r [23] are

$$\mu_r = \sqrt{2\sigma^2} e^{-\frac{s^2}{2\sigma^2}} \sum_{k=0}^{\infty} \frac{\Gamma(k+\frac{3}{2})}{k!k!}(\frac{s^2}{2\sigma^2})^k \qquad (3.14)$$

$$\sigma_r^2 = 2\sigma^2 e^{-\frac{s^2}{2\sigma^2}} \sum_{k=0}^{\infty} \frac{k+1}{k!}(\frac{s^2}{2\sigma^2})^k - \mu_r^2. \qquad (3.15)$$

3.2   Classification of Channels

The impulse response of mobile radio channel exhibits time delay and doppler spreading. Time delay results in time dispersion and frequency-selective fading . Doppler spreading results in frequency dispersion and time-selective fading. These two cases are discussed below [24].

3.2.1   Time Dispersion and Frequency Selective Fading Channel

The coherence bandwidth B_c of the channel is related to the multipath spread τ. Multipath spread describes the time spread of the received signal in the time domain

because of the multipath effect. The relation between B_c and τ is

$$B_c = \frac{1}{2\pi\tau} \tag{3.16}$$

If the bandwidth B_x of the transmitted signal is sufficiently less than the coherent bandwidth B_c of the channel, all frequency components of the transmitted signal will receive approximately the same attenuation, there is no frequency selective fading, and the channel is termed frequency non-selective.

Otherwise, if B_x is larger than B_c, the frequency components at the edge of the spectrum will be attenuated differently, hence there is a frequency selective fading, and the channel is frequency selective.

3.2.2   Frequency Dispersion and Time Selective Fading Channel

The coherence time T_c of the channel is related to the the Doppler spread B_d, that is

$$T_c = \frac{1}{B_d} \tag{3.17}$$

If the duration time T_x of the transmitted signal is sufficiently less than the coherent time T_c of the channel, The signal will pass through the channel before any significant change in its characteristics. The channel can be considered as time invariant, thus, the channel can be called as a time non-selective channel. In the frequency domain, the bandwidth of the signal is much larger than the Doppler spread, so the influence of the Doppler spread is ignored. The channel is also called no frequency dispersion channel.

Otherwise, if T_x is larger than T_c, the characteristics of the channel will change while the signal is going through the channel. The channel is time variant and the signal suffer time selective fading. The channel can be considered as a time selective channel.

When T_x is very large, the Doppler spread of the signal becomes large relative to

the signal's bandwidth. The received spectrum of the signal will be able to observe distinct widening, and the channel is also called frequency dispersion channel.

CHAPTER 4

OFDM-CDMA

Multicarrier modulation or orthogonal frequency division multiplexing(OFDM) has drawn a lot of attention in the field of mobile communications. This is mainly because of the need to transmit high data rate in the narrow-band wireless communication systems. Code Division Multiple Access(CDMA) is a multiplexing technique where many users can simultaneously and asynchronously access a channel by modulation and spreading their information. The combination of OFDM with CDMA (OFDM-CDMA) [11, 12] is an interesting method for the mobile communication systems. OFDM-CDMA also inherits the disadvantage of the OFDM system, high PAPR. In this chapter, OFDM-CDMA model is discussed first, then some methods are used to reduce PAPR in OFDM-CDMA.

4.1 OFDM-CDMA System Model

The whole OFDM-CDMA system model with coding technique is illustrated in [11, 12] Figure 4.1. For simplicity, only one user case is shown here.

The downlink OFDM-CDMA system consists of three parts, that is, the transmitter at the base station, the mobile channel and the receiver at the mobile station. These three parts will be discussed in detail in the following section.

4.2 Transmitter model

The transmitter model [11, 12] is illustrated in Figure 4.2. In this model, the IFFT operator is used for multicarrier modulation. The input data $d_k(i)$ is assumed to be a binary antipodal signal, where $k = 1, 2, \cdots, K$. Here, $d_k(i)$ denotes the i bit of a serial to parallel converting sequence for the user k. $d_k(i)$ is assumed to be either 1
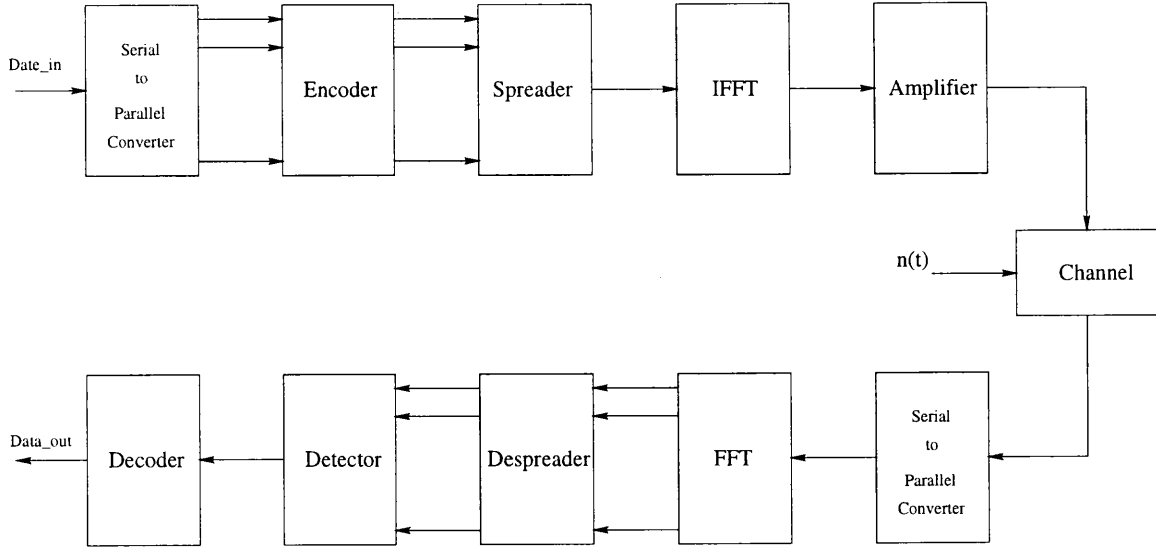
Figure 4.1 Block Diagram of OFDM-CDMA System Model

or -1 with the same probability. The transmitter can be expressed in the following steps.

1. A serial input data sequence from the user k is

$$d_k(t) = \sum_{i=1}^{\infty} \sqrt{P_k} d_k(i) P(t - iT_d) \tag{4.1}$$

where P(t) is a rectangular pulse with the bit time duration T_d and P_k is the power of the user k.

After a one-to-M Serial to Parallel Converter, the input data can be written as a vector $\mathbf{d_k} = [d_k(1), d_k(2), \cdots, d_k(M)]$ before the encoder block. The element of $\mathbf{d_k}$, $d_k(m)$ can be expressed as

$$d_k(m)(t) = \sum_{i=1}^{\infty} \sqrt{P_k} d_k(m) P(t - iT_b) \quad m = 1, 2, \cdots, M \tag{4.2}$$

where $T_b = M \times T_d$. Thus the duration of the input data are spread to overcome the delay spread of the channel, and the net bit rate is unchanged, as M bits are transfered simultaneously during T_b.
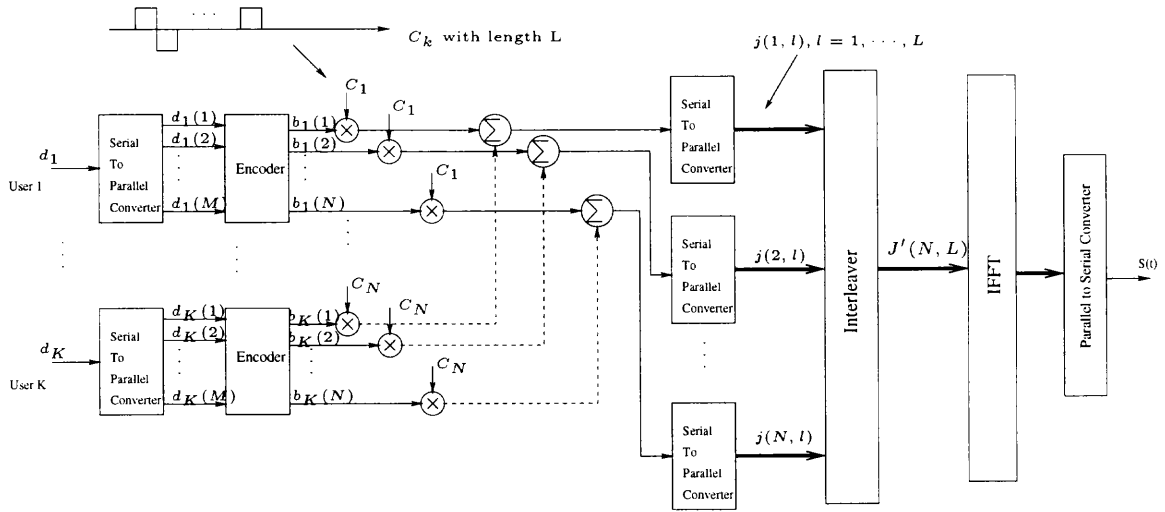
Figure 4.2 Block Diagram of OFDM-CDMA Transmitter Model

2. The encoder in Figure 4.1 uses coding techniques discussed in chapter 2 to encode the input data $d_k(m), m = 1, 2, \cdots, M$. Because of the addition of the redundancy, the output vector of the encoder $\mathbf{b_k}$ is larger than $\mathbf{d_k}$; $\mathbf{b_k} = [b_k(1), b_k(2), \cdots, b_k(N)]$, whose length is $N > M$. The element of $\mathbf{b_k}$, $b_k(n)$ can be expressed as

$$b_k(n)(t) = \sum_{i=1}^{\infty} \sqrt{P_k} b_k(n) P(t - iT_b) \quad n = 1, 2, \cdots, N \tag{4.3}$$

3. After the encoder, each symbol $b_k(n)$ from the user k is spread by the user-specific sequence $C_k = [c_k(1), c_k(2), \cdots, c_k(L)]$. C_k can be expressed as

$$c_k(t) = \sum_{l=1}^{L} c_k(l) P(t - lT_c) \tag{4.4}$$

where L is the length of the spreading code and T_c is the time duration of the chip and $T_b = L \times T_c$. The output of the the multiplier, $\mathbf{x_k} = [x_k(1), x_k(2), \cdots, x_k(N)]$ can be expressed as

$$x_k(n)(t) = \sum_{i=1}^{\infty} \left(\sum_{l=1}^{L} \sqrt{P_k} b_k(n) c_k(l) P(t - lT_c) \right) P(t - iT_b) \tag{4.5}$$

Both $b_k(n)$ and $x_k(n)$ are shown in Figure 4.3.
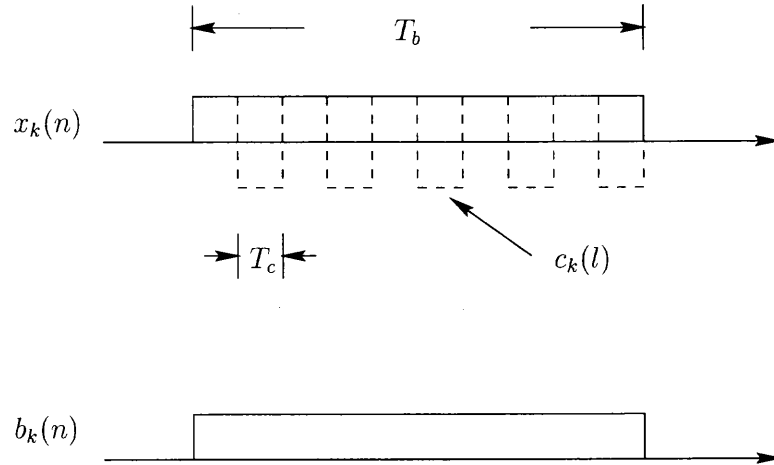
Figure 4.3 Diagram of Waveforms of the Signal

4. Using different spreading codes, different output, $\mathbf{x_k}$ from different users can be summed for transmission. The output of the sum can expressed as a vector $\mathbf{x'}= [x'(1), x'(2), \cdots, x'(N)]$, where $x'(n)$ is

$$x'(n)(t) = \sum_{i=1}^{\infty} (\sum_{l=}^{L} (\sum_{k=1}^{K} \sqrt{P_k} b_k(n) c_k(l)) P(t - lT_c)) P(t - iT_b) \qquad (4.6)$$

5. Before the multicarrier modulation, each chip of the signal has to be spread in the time domain to be the bit time T_b. A one-to-L serial to parallel converter is used for this purpose. The output of the converter can be expressed as a vector

$$\mathbf{j(N, L)} = [j(1,1), j(1,2), \cdots, j(1,L), j(2,1), j(2,2), \cdots, j(2,L),$$
$$\cdots\cdots, j(N,1), j(N,2), \cdots, j(N,L)] \qquad (4.7)$$

Where $j(n,l)$ is

$$j(n,l)(t) = \sum_{i=1}^{\infty} \sum_{k=1}^{K} \sqrt{P_k} b_k(n) c_k(l) P(t - iT_b) \qquad (4.8)$$

For $n = 1, 2, \cdots, N$ and $l = 1, 2, \cdots, L$

6. In order to scramble the symbols to achieve independent fading by the channel. A N-input block interleaver with depth L is used. A block interleaver formats

Output
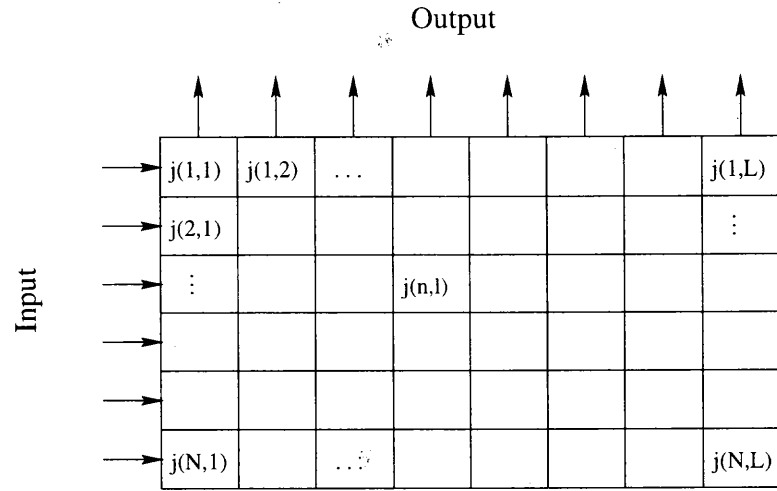
Figure 4.4 Block Diagram of Block Interleaver

the data in rectangular array of N rows and L columns. Each row of the array constitutes a code word of length L. This interleaver is illustrated in Figure 4.4 . The symbols are read out column-wise and transmitted over the channel. In order to recover the data at the receiver, a deinterleaver is used . The deinterleaver stores the data in the same rectangular array format, but it is read out row-wise, one code word at a time. The output of the interleaver can be expressed as a vector

$$
\begin{aligned}
\mathbf{j}'(\mathbf{N}, \mathbf{L}) \; = \; & [j(1,1), j(2,1), \cdots, i(N,1), j(1,2), j(2,2), \cdots, j(N,2), \\
& \cdots\cdots, j(1,L), j(2,L), \cdots, j(N,L)]
\end{aligned}
\tag{4.9}
$$

7. The IFFT of size LN modulates each data onto different frequency carriers. The modulated signal at each frequency bin, $S(m')$, used for transmission is

$$
\begin{aligned}
S(m')(t) \; = \; & \sum_{i=1}^{\infty}\sum_{l=1}^{L}\sum_{n=1}^{N}(\sum_{k=1}^{K}\sqrt{P_k}b_k(n)c_k(l))e^{j2\pi\{N(l-1)+(n-1)\}\frac{m'}{NL}}P(t-iT_b) \\
= \; & \sum_{i=1}^{\infty}\sum_{q=0}^{L\times N-1}(\sum_{k=1}^{K}\sqrt{P_k}b_k(n)c_k(l))e^{j2\pi q\frac{m'}{NL}}P(t-iT_b)
\end{aligned}
\tag{4.10}
$$

where $q = N(l-1)+(n-1), n = 1, \cdots, N$ and $l = 1, \cdots, L$.

8. Converting the discrete version of the modulated signal into a continuous version, we get for the transmitted signal $S(t)$;

$$S(t) = \sum_{i=1}^{\infty} \sum_{q=0}^{L \times N-1} (\sum_{k=1}^{K} \sqrt{P_k} b_k(n) c_k(l)) e^{j2\pi q \frac{t}{T_b}} P(t - iT_b) \qquad (4.11)$$

4.3　Channel Model

Using the channel models discussed in Chapter 2, we establish the channel model for OFDM-CDMA system. If the the time duration $T_b = M \times T_d$ of the transmitted signal is much smaller than the coherent time T_c of the channel, then the channel can be assumed as a time-invariant channel and the doppler shift is ignored. After OFDM modulation, because the bandwidth of each subcarrier $B_b = \frac{1}{T_b}$ is much smaller than the coherent bandwidth B_c of the channel. Each Different subcarrier will suffer independent fading and the channel is assumed as a non-frequency selective channel. From a frequency-domain viewpoint, the frequency response of the channel at the subcarrier frequencies $f(j') = \frac{j'}{T_b}$ is [23]

$$H'(j') = \sum_{i=0}^{NL-1} h(i') e^{-j2\pi \frac{i'j'}{NL}} \qquad j' = 0, 1, \cdots, NL - 1 \qquad (4.12)$$

Where $h(i')$,$i' = 0, 1, \cdots, NL - 1$ is the sampled channel impulse response.

4.4　Receiver model

The receiver scheme is illustrated in Figure 4.5.　If we consider one time duration T_b for the received signal, then the receiver can be expressed in the following steps.

1. The input signal at the receiver, $R(t)$ is

$$R(t) = S(t) * h(t) + n(t) \qquad (4.13)$$

Block Diagram of OFDM-CDMA Receiver
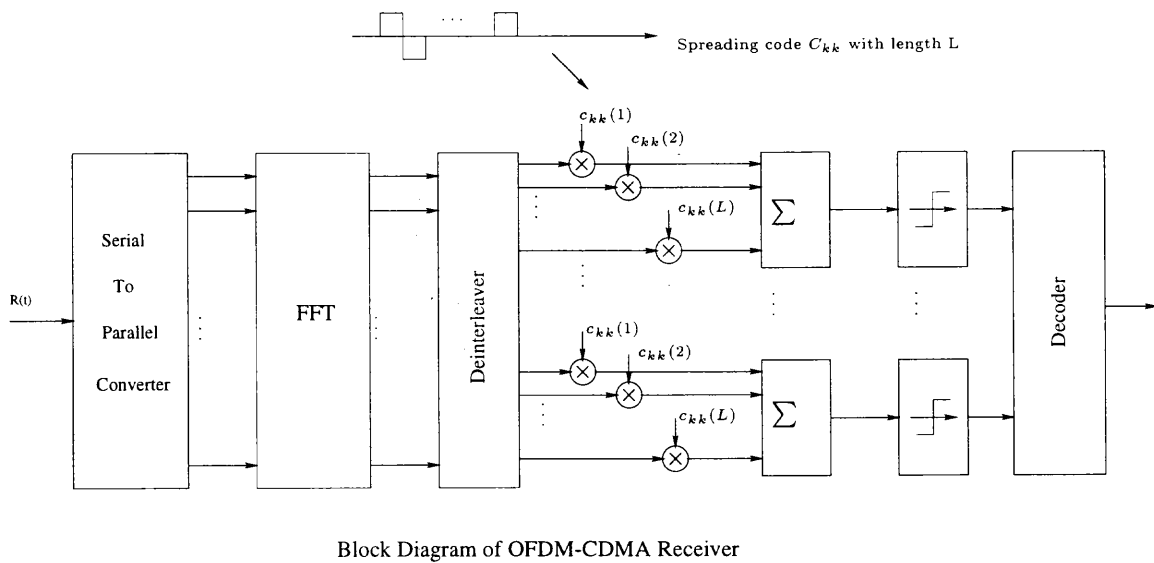
Figure 4.5 Block Diagram of OFDM-CDMA Receiver Model for User kk

where $*$ denotes convolution, h(t) is the channel impulse response function and $n(t)$ denotes the additive white Gaussian noise with zero mean and variance σ^2.

2. At the serial to parallel block, the received signal is sampled and converted into a parallel form. The output can be expressed as

$$R(p) = S(p) * h(p) + n(p) \quad p = 0, 1, \cdots, NL - 1 \tag{4.14}$$

Where h(p) is the sampled channel impulse response. Substituting $S(p)$ with Equation(4.10), $R(p)$ is

$$R(p) = \sum_{q=0}^{L \times N - 1} (\sum_{k=1}^{K} \sqrt{P_k} b_k(n) c_k(l)) e^{j2\pi \frac{pq}{NL}} * h(p) + n(p) \tag{4.15}$$

Let $d'(q) = \sum_{k=1}^{K} \sqrt{P_k} b_k(n) c_k(l) \quad q = N(l - 1) + (n - 1), n = 1, 2, \cdots, N,$ $l = 1, 2, \cdots, L$ and $q = 0, 1, \cdots, NL - 1$. $R(p)$ can be expressed as

$$R(p) = \sum_{q=0}^{L \times N - 1} d'(q) e^{j2\pi \frac{pq}{NL}} * h(p) + n(p) \quad p = 0, 1, \cdots, NL - 1 \tag{4.16}$$

$$= IFFT\{d'(q)\} * h(p) + n(p) \tag{4.17}$$

3. Using the similar mathematical derivation method from Equation (2.4) to Equation (2.5) in Chapter 2, $R(p)$ can be expressed as

$$
\begin{aligned}
R(p) &= \sum_{q=0}^{L\times N-1} d'(q)e^{j2\pi\frac{pq}{NL}} * h(p) + n(p) \\
&= \sum_{m=0}^{NL-1}\sum_{q=0}^{L\times N-1} d'(q)e^{j2\pi\frac{mq}{NL}} h(p-m) + n(p) \\
&= \sum_{q=0}^{L\times N-1} d'(q)\sum_{m=0}^{NL-1} e^{j2\pi\frac{mq}{NL}} h(p-m) + n(p) \\
&= \sum_{q=0}^{L\times N-1} d'(q)[e^{j2\pi\frac{mq}{NL}} * h(m)] + n(p) \\
&= \sum_{q=0}^{L\times N-1} d'(q)\sum_{m'=0}^{NL-1} e^{j2\pi\frac{(p-m')q}{NL}} h(m') + n(p) \\
&= \sum_{q=0}^{L\times N-1} d'(q)[\sum_{m'=0}^{NL-1} h(m')e^{-j2\pi\frac{m'q}{NL}}]e^{j2\pi\frac{pq}{NL}} \\
&= \sum_{q=0}^{L\times N-1} d'(q)H'(q)e^{j2\pi\frac{pq}{NL}} + n(p) \\
&= IFFT\{d'(q)H'(q)\} + n(p) \\
&= IFFT\{(\sum_{k=1}^{K} \sqrt{P_k}b_k(n)c_k(l))H'(q)\} + n(p) \qquad (4.18)
\end{aligned}
$$

Where $q = 0, 1, \cdots, NL - 1$ and $H'(q)$ is the frequency response of the channel at the subcarrier frequencies given in Equation (4.12).

4. To demodulate the signal, the FFT transformation is used. The output is a vector $\mathbf{r} = [r(0), r(1), \ldots, r(NL-1)]^T$, where $r(u) \quad u = 0, 1, \cdots, NL - 1$ is

$$
\begin{aligned}
r(u) &= FFT\{R(p)\} \\
&= (\sum_{k=1}^{K} \sqrt{P_k}b_k(n)c_k(l))H'(u) + \xi(u) \qquad (4.19)
\end{aligned}
$$

Where $n = 1, 2, \cdots, N$, $l = 1, 2, \cdots, L$ and $u = 0, 1, \cdots, NL - 1$. $\xi(u)$ is the additive white Gaussian noise with zero mean and variance σ_u^2.

5. The vector **r** has to be deinterleaved after FFT block. The resultant vector for this operation is a vector

$$
\mathbf{y} = [y(1,1), y(1,2), \cdots, y(1,L), y(2,1), y(2,2), \cdots,
$$

$$
y(2,L), \cdots, y(N,1), y(N,2), \cdots, y(N,L)]^T \tag{4.20}
$$

Where $y(n,l) = \sum_{k=1}^{K} \sqrt{P_k} b_k(n) c_k(l) H'(n,l) + \xi(n,l)$ and

$y(n,l) = r((l-1)N + n - 1) \quad n = 1,\ldots,N \quad l = 1,\ldots,N,$

$H'(n,l) = H'((l-1)N + n - 1) \quad n = 1,\ldots,N \quad l = 1,\ldots,N,$

$\xi(n,l) = \xi((l-1)N + n - 1) \quad n = 1,\ldots,N \quad l = 1,\ldots,N.$

6. After the deinterleaver, the vector **y** will be multiplied by the spreading code $C_{kk} = [c_{kk}(1), c_{kk}(2), \cdots, c_{kk}(L)]$ for the specific user kk, and then the sum is sent for the detection. The output of the summation can be expressed as a vector $\mathbf{b'} = [b'_{kk}(1), b'_{kk}(2), \ldots, b'_{kk}(N)]$.

$b'_{kk}(n)$ can be expressed as

$$
\begin{aligned}
b'_{kk}(n) &= \sum_{l=1}^{L} y(n,l) c_{kk}(l) \\
&= \sum_{l=1}^{L} \left\{ \sum_{k=1}^{K} \sqrt{P_k} b_k(n) c_k(l) H'(n,l) + \xi(n,l) \right\} c_{kk}(l) \\
&= \sum_{l=1}^{L} \sqrt{P_{kk}} b_{kk}(n) c_{kk}^2(l) H'(n,l) + \sum_{l=1}^{L} \sum_{k=1,k\neq kk}^{K} \sqrt{P_k} b_k(n) c_k(l) c_{kk}(l) H'(n,l) \\
&\quad + \sum_{l=1}^{L} \xi(n,l) c_{kk}(l)
\end{aligned} \tag{4.21}
$$

Where the first item includes the desired information, the second item includes the interference from different users and the last item represents the noise.

7. The estimated bit vector $\hat{\mathbf{b}}$ for the user kk can be expressed as

$$
\hat{\mathbf{b}} = sign(\mathbf{b'}) \tag{4.22}
$$

Considering Rayleigh fading channel effect, the second item in Equation (4.21) can't be cancelled by despreading. Some modification has to be made in the receiver to

cancel the multiuser interference. Here a conventional decorrelator [25] is used in the simulation, which will be discussed using the matrix notation in the following section. The resultant $\mathbf{z}$ from the decorrelator can be used to estimate the transmitted bit. That estimated bit $\hat{\mathbf{b}}$ is

$$\hat{\mathbf{b}} = sign(\mathbf{z}) \tag{4.23}$$

4.5 Matrix Notation of OFDM-CDMA Model

In the last section, the OFDM-CDMA system was presented in regular mathematic notation. In order to simulate the whole system with all users clearly we turn to the matrix notation. The reason for the matrix notation is that we can use computer to simulate OFDM-CDMA system much easier.

1. Consider the number of users is K, the output of the encoder $\mathbf{b}$ can be expressed as

$$\mathbf{b} = \begin{bmatrix} b_1(1) \\ b_2(1) \\ \vdots \\ b_K(1) \\ \vdots \\ b_1(N) \\ b_2(N) \\ \vdots \\ b_K(N) \end{bmatrix}_{KN \times 1}$$

The matrix of the power of different users can be expressed as a $KN \times KN$ diagonal matrix. That is

$$\mathbf{P} = \begin{bmatrix} \sqrt{P_K} & 0 & \cdots & 0 \\ 0 & & \cdots & 0 \\ \vdots & \vdots & \ddots & \vdots \\ 0 & 0 & \cdots & \sqrt{P_K} \end{bmatrix}_{KN \times KN}$$

Where $\mathbf{P_K}$ can be expressed as

$$\mathbf{P_K} = \begin{bmatrix} \sqrt{P_1} & 0 & \cdots & 0 \\ 0 & \sqrt{P_2} & \cdots & 0 \\ \vdots & \vdots & \ddots & \vdots \\ 0 & 0 & \cdots & \sqrt{P_K} \end{bmatrix}_{\mathbf{K \times K}}$$

For total K users, there are K different user-specific sequence C_k. The length of the sequence is L. The user-specific sequence $\mathbf{c}$ can be expressed as

$$\mathbf{c} = \begin{bmatrix} c_1(1) & c_1(2) & \cdots & c_1(L) \\ c_2(1) & c_2(2) & \cdots & c_2(L) \\ \vdots & \vdots & \ddots & \vdots \\ c_K(1) & c_K(2) & \cdots & c_K(L) \end{bmatrix}_{\mathbf{K \times L}}$$

Then from the matrix $\mathbf{c}$, a new matrix of the spreading sequence can be expressed as

$$\mathbf{C} = \begin{bmatrix} \mathbf{c} & 0 & \cdots & 0 \\ 0 & \mathbf{c} & \cdots & 0 \\ \vdots & \vdots & \ddots & \vdots \\ 0 & 0 & \cdots & \mathbf{c} \end{bmatrix}_{\mathbf{KN \times LN}}$$

2. After the spreader, the output N-parallel and L-serial symbols from different users are added together correspondingly, then the resultant vector $\mathbf{i}$ is

$$\mathbf{i} = \mathbf{C^T P b} \tag{4.24}$$

That is

$$\mathbf{i} = \begin{bmatrix} \sum_{k=1}^{K} \sqrt{P_k} b_k(1) c_k(1) \\ \sum_{k=1}^{K} \sqrt{P_k} b_k(1) c_k(2) \\ \vdots \\ \sum_{k=1}^{K} \sqrt{P_k} b_k(1) c_k(L) \\ \vdots \\ \sum_{k=1}^{K} \sqrt{P_k} b_k(N) c_k(1) \\ \sum_{k=1}^{K} \sqrt{P_k} b_k(N) c_k(2) \\ \vdots \\ \sum_{k=1}^{K} \sqrt{P_k} b_k(N) c_k(L) \end{bmatrix}_{\mathbf{LN \times 1}}$$

Because of the deinterleaver at the receiver, the effect of the interleaver on the transmitted signal is ignored. Therefore, after a serial to parallel converter, the resultant signal vector is also $\mathbf{i}$.

3. The channel frequency response $H'(n, l)$ can be expressed as a matrix $\mathbf{H}$. that is

$$\mathbf{H} = \begin{bmatrix} H'(1,1) & 0 & \cdots & 0 & 0 & 0 & 0 \\ 0 & \ddots & 0 & \cdots & 0 & 0 & 0 \\ 0 & 0 & H'(1,L) & 0 & \cdots & 0 & 0 \\ \vdots & \vdots & \vdots & \ddots & \vdots & \vdots & \vdots \\ 0 & \cdots & 0 & 0 & H'(N,1) & 0 & 0 \\ \vdots & \vdots & \vdots & \vdots & \vdots & \ddots & \vdots \\ 0 & 0 & \cdots & \cdots & 0 & 0 & H'(N,L) \end{bmatrix}_{NL \times NL}$$

The AWGN noise can be expressed as a noise vector $\mathbf{n}$. That is

$$\mathbf{n} = \begin{bmatrix} \xi(1,1) \\ \vdots \\ \xi(1,L) \\ \vdots \\ \xi(N,1) \\ \vdots \\ \xi(N,L) \end{bmatrix}_{NL \times 1}$$

From Equation (4.20), it can be seen that at the receiver, the vector Y can be expressed as

$$\mathbf{y} = \mathbf{Hi} + \mathbf{n} \tag{4.25}$$

4. From Equation (4.21), the estimation of the received bit b' can be expressed as a vector $\mathbf{b}'$, that is

$$\mathbf{b}' = \begin{bmatrix} b'_1(1) \\ b'_2(1) \\ \vdots \\ b'_K(1) \\ \vdots \\ b'_1(N) \\ b'_2(N) \\ \vdots \\ b'_K(N) \end{bmatrix}_{KN \times 1}$$

It can be seen that

$$\mathbf{b}' = \mathbf{Cy}$$

$$= \mathbf{CHC^TPb} + \mathbf{Cn} \qquad (4.26)$$

5. In order to cancel the multiuser interference, a conventional decorrelator is used here. First, a cross-correlation matrix $\mathbf{Q}$ is defined as

$$\mathbf{Q} = \mathbf{CHC^T} \qquad (4.27)$$

In order to separate the interference from other users completely, The inverse matrix of $\mathbf{Q}$ is used for decorrelation. That is the estimation of the transmitted bit is

$$\hat{\mathbf{b}} = sign(\mathbf{z}) \qquad (4.28)$$

Where $\mathbf{z} = \mathbf{Q^{-1}b'}$

4.6   Spreading Sequence

In order to separate the bits from different user, spreading sequences are used. Here, two orthogonal sets of sequences are discussed.

4.6.1   Walsh-Hadamard(WH) Sequence

The Walsh-Hadamard sequences can be recursively obtained by

$$\mathbf{C_{2L}^W} = \begin{bmatrix} \mathbf{C_L^W} & \mathbf{C_L^W} \\ \mathbf{C_L^W} & -\mathbf{C_L^W} \end{bmatrix}$$

and

$$\mathbf{C_2^W} = \frac{1}{\sqrt{2}} \begin{bmatrix} 1 & 1 \\ 1 & -1 \end{bmatrix}$$

For example, when $L = 2$, the WH sequence is

$$\mathbf{C_4^W} = \begin{bmatrix} C_1 \\ C_2 \\ C_3 \\ C_4 \end{bmatrix} = \frac{1}{\sqrt{4}} \begin{bmatrix} 1 & 1 & 1 & 1 \\ 1 & -1 & 1 & -1 \\ 1 & 1 & -1 & -1 \\ 1 & -1 & -1 & 1 \end{bmatrix}$$

It can be seen that $C(i)$ are orthogonal with each other.

4.6.2 Complementary(CP) Sequence

In a similar manner, an orthogonal set of Golay complementary sequences can be recursively obtained by

$$\mathbf{C_{2L}^C} = \begin{bmatrix} \mathbf{C_L^C} & \mathbf{\bar{C}_L^C} \\ \mathbf{C_L^C} & -\mathbf{\bar{C}_L^C} \end{bmatrix}$$

and

$$\mathbf{C_2^C} = \frac{1}{\sqrt{2}} \begin{bmatrix} 1 & 1 \\ 1 & -1 \end{bmatrix}$$

where $\mathbf{\bar{C}_L^C}$ is composed of $\mathbf{C_L^C}$ of which the right half columns are reversed, e.g., if $\mathbf{C_L^C} = \begin{bmatrix} \mathbf{A_L} & \mathbf{B_L} \end{bmatrix}$ where $\mathbf{A_L}$ and $\mathbf{B_L}$ are $L \times \frac{L}{2}$ matrices, then $\mathbf{\bar{C}_L^C} = \begin{bmatrix} \mathbf{A_L} & -\mathbf{B_L} \end{bmatrix}$

For example, when $L = 2$, the CP sequence is

$$\mathbf{C_4^C} = \begin{bmatrix} C_1 \\ C_2 \\ C_3 \\ C_4 \end{bmatrix} = \frac{1}{\sqrt{4}} \begin{bmatrix} 1 & 1 & 1 & -1 \\ 1 & -1 & 1 & 1 \\ 1 & 1 & -1 & 1 \\ 1 & -1 & -1 & -1 \end{bmatrix}$$

It can be seen that

$$\mathbf{C_L^C} \cdot \mathbf{C_L^{C^T}} = \mathbf{I_L} \tag{4.29}$$

where $\mathbf{I_L}$ denotes the $L \times L$ identity matrix, so the matrix given above is orthogonal, and each row is composed of Golay binary complementary sequence.

4.7 Simulation of PAPR Reduction in OFDM-CDMA System

In OFDM-CDMA system, High PAPR is also a main disadvantage. Here, coding schemes discussed in Chapter 2 will be used in OFDM-CDMA system. The spreading sequence is used with WH,CP and Gold code. Gaussian non-fading channel and Rayleigh fading channel are used in the simulation. It can be seen that a better performance is achieved when using these methods, especially the block coding scheme with bit position control.

4.7.1 Simulations with Walsh-Hadamard Sequence and Complementary Sequence as the Spreading Sequence in Gaussian channel

In this simulation, Walsh-Hadamard sequence and Complementary Sequence are used as the spreading sequence. The length of the WH sequence and the CP sequence is $L = 8$, and the length of the code word after the encoder is $N = 8$, thus the number of the multicarriers is totally 64. The largest user number which is determined by L can be 8. Because there are 64 multicarriers, the largest PAPR is 64 when only one user is considered. More users could increase PAPR. The clipping level is 10dB. When the amplitude of an OFDM signal is larger than 10dB, the amplitude will be clipped to 10dB before transmission. The phase of the signal keeps unchanged. Thus the clipping distortion will be produced. In these simulations,we chose the number of users $k = 4$. The channel is Gaussian non-fading channel. Because of the orthogonality of the spreading sequences, there is no multiuser interference.
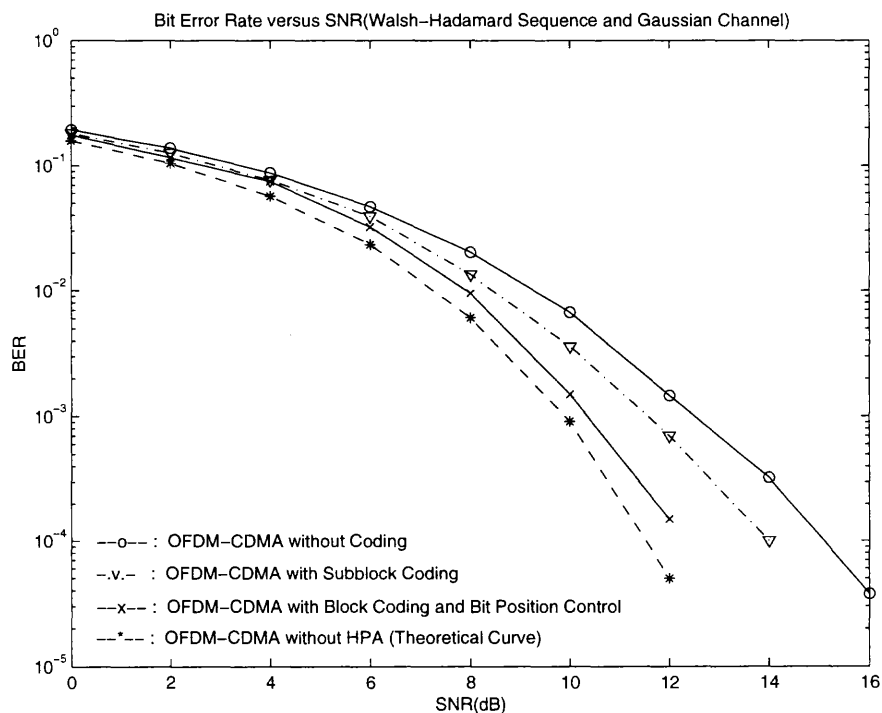
Figure 4.6 Block Diagram of BER Versus SNR in OFDM-CDMA with WH Spreading Sequence

It is shown in Figure 4.6 and Figure 4.7 that for the same SNR, BER is lower

for the block coding scheme with bit position control. This is due to the PAPR reduction effect. This curve is very near to the theoretical curve without HPA clipping influence. BER for the same SNR using subblock coding scheme is lower than BER with HPA clipping and without any coding scheme, but larger than BER with the block coding scheme having bit position control. Therefore, the novel block coding scheme has a better performance in OFDM-CDMA system compared with previously proposed block coding scheme.
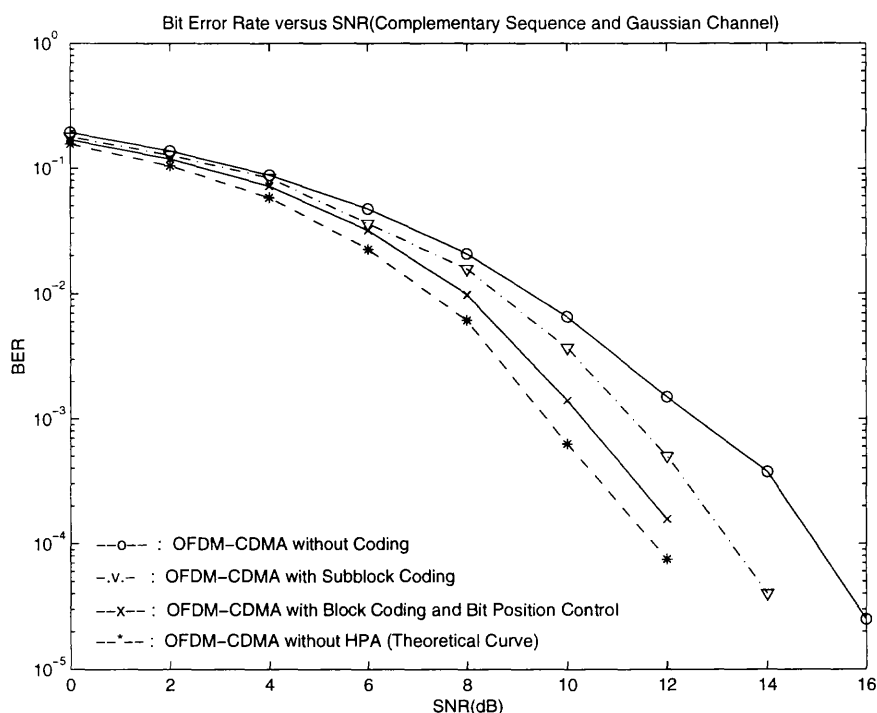
Figure 4.7 Block Diagram of BER Versus SNR in OFDM-CDMA with CP Spreading Sequence

4.7.2 Simulations with Gold Code as the Spreading Sequence in Gaussian Channel

We use the same conditions as the last section for simulations except for implementing Gold code as the spreading sequence. That is $N = 8$ and $K = 4$, clipping level is 10dB and the length of the Gold code is $L = 7$. Because the Gold code is not orthogonal, there exists multiuser interference. A conventional decorrelator to cancel

the multiuser interference in the simulation.

Different coding schemes are also used in the simulation. The results are shown in Figure 4.8. It is shown that the block coding scheme using bit position control has a better system performance even though the multiuser interference exists.

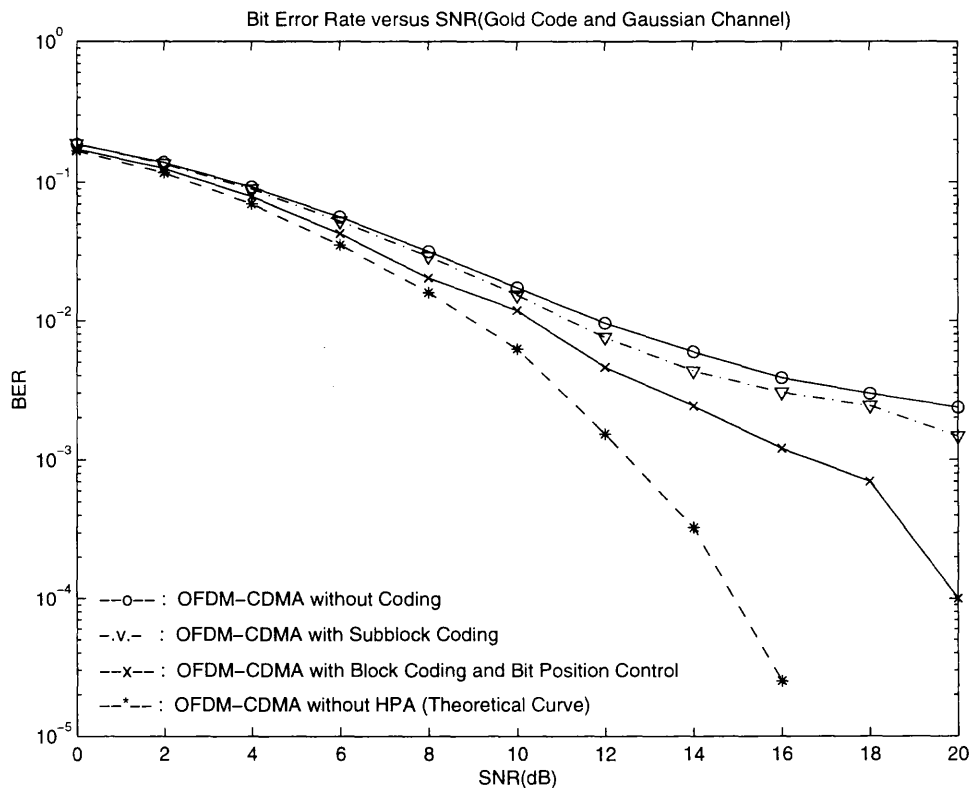
Figure 4.8 Block Diagram of BER Versus SNR in OFDM-CDMA with Gold Code

4.7.3 Simulations with Gold Code as the Spreading Sequence in Rayleigh Fading Channel

In this simulation, we use Rayleigh fading channel. Gold code is used as the spreading sequence. The length of the Gold code is $L = 7$. $N = 8$ and $K = 4$ and the clipping level is 10dB. Clearly there exists multiuser interference. Here we use a conventional decorrelator to cancel the multiuser interference. Simulation results are shown in Figure 4.9. It is shown that using Rayleigh fading channel, the block coding scheme

using bit position control has a better system performance than previously proposed block coding scheme.
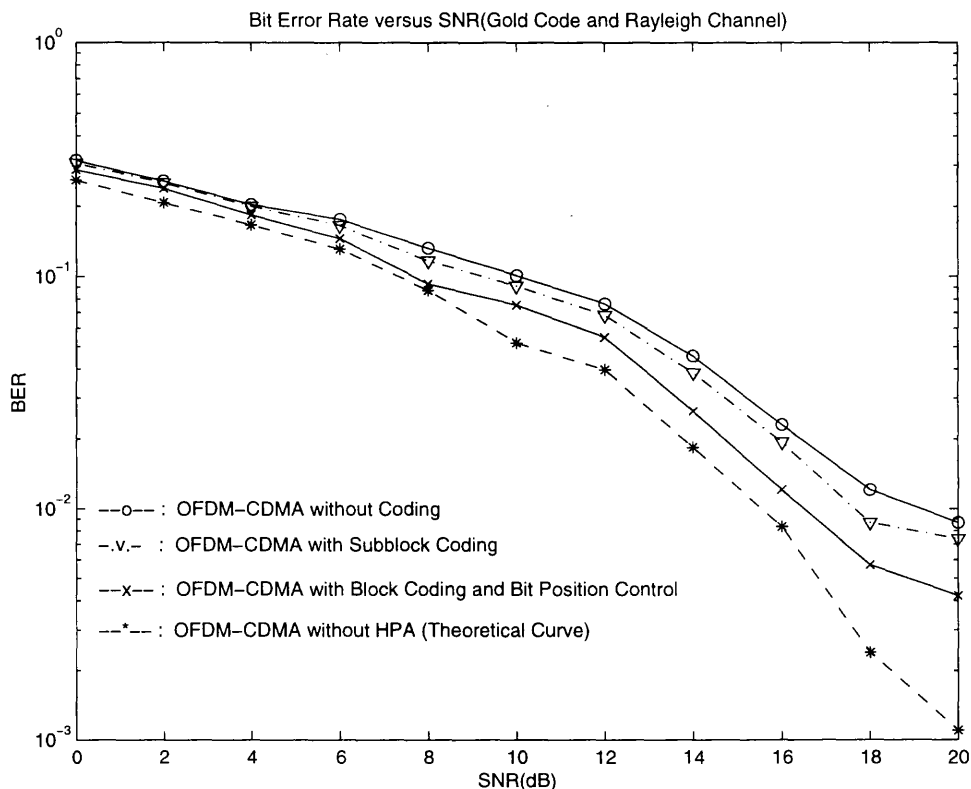
Figure 4.9 Block Diagram of BER Versus SNR in OFDM-CDMA through Rayleigh Channel

4.7.4 BER Improvement Comparison in different Channels

In this section, BER improvement with the new coding scheme is compared between Gaussian non-fading channel and Rayleigh fading channel. After comparing the simulation results from Section 4.7.2 and Section 4.7.3, It is shown in Figure 4.10 that BER improvement in Rayleigh fading channel is better than that in Gaussian channel.
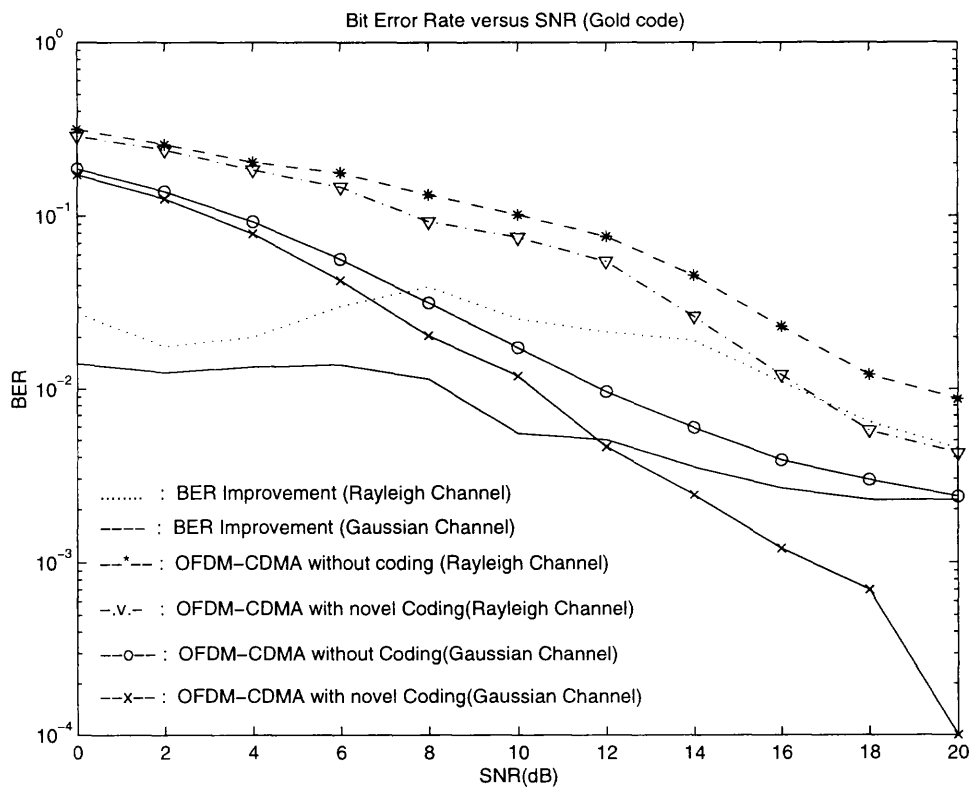
Figure 4.10 Block Diagram of BER Improvement

CHAPTER 5

CONCLUSION

In this thesis, reduction of Peak to Average Power Ratio in OFDM and OFDM-CDMA system is discussed.

In OFDM system, a compensated High Power Amplifier linear plus clipping is used in the simulation. Clipping effect is also considered in the performance evaluation. When the new block coding with bit position control is used, PAPR is reduced significantly compared to other block coding schemes, suggested previously in literatures. In fact, using previously proposed block coding schemes for the same signal to noise ratio, the bit error rate can't be improved much compared with BER without coding. However, with the novel block coding scheme, BER can be decreased significantly almost to level obtained without clipping. This is due to the less clipping distortion when PAPR is reduced.

In OFDM-CDMA system, the orthogonal or non-orthogonal spreading sequences are used to distinguish data from different users. Gaussian channel and Rayleigh channel are used as the channel model. OFDM-CDMA also inherits the high PAPR disadvantage from OFDM modulation. The coding schemes discussed in OFDM system are also used in OFDM-CDMA. The spreading sequences are chosen as Walsh-Hadamard, Complementary or Gold code sequences. The code words are encoded before spreading. It can be seen that coding schemes can also reduce PAPR in OFDM-CDMA despite the fact that spreading processes change the actual code words for OFDM modulation. With the novel block coding scheme performance is significantly better than with previously proposed block coding schemes no matter WH, CP or Gold code sequences are used.

REFERENCES

1. Bingham, John A.C, "Multicarrier modulation for data transmission: An idea whose time has come Bingham, John A.C. Author" *IEEE Communications Magazine, vol. 28, pp. 5-14, May 1990.*

2. Shinsuke Hara and Ramjee Prasad, "Overview of Multicarrier CDMA", *IEEE Communication Magazine, pp.126-133, December 1997.*

3. D.Wulich and L.Goldfeld, " Reduction of Peak Factor in Orthogonal Multicarrier Modulation by Amplitude Limiting and Coding" *IEEE transactions on communications, Vol. 47, No. 1, pp. 18-21, January 1999.*

4. A.E. Jones, T.A.Wilkinson and S.K. Barton,"Block coding scheme for reduction of peak to mean envelope power ratio of multicarrier transmission schemes", *Electronics Letters, vol.30, pp. 2098-2099, 1994.*

5. Fragiacomo, S., Matrakidis, C. and O'Reilly, J.J,"Multicarrier transmission peak-to-average power reduction using simple block code", *Electronics Letters, vol. 34, pp. 953-954, May 1998.*

6. Li, Xiaodong; Ritcey, J.A., "M-sequences for OFDM peak-to-average power ratio reduction and error correction", *Electronics Letters, vol. 33, pp. 554-555, Mar. 1997.*

7. T.A. Wilkinson and A.E. Jones, "Minimization of the Peak to Mean Envelope Power Ratio in Multicarrier Transmission Schemes by Block coding", *Proc. IEEE VTC95, Chicago, pp. 825-831, Jul 1995.*

8. J.A. Davis and J. Jedwab, "Peak-to-mean power control and error correction for OFDM transmission using Golay sequences and Reed-Muller codes" *Electronics Letters, vol. 33, pp. 267-268, Feb. 1997.*

9. van Nee, Richard D.J., "OFDM codes for peak-to-average power reduction and error correction", *IEEE Global Telecommunications Conference, vol. 1, pp. 740-744, Nov. 1996.*

10. Branislav M. Popovic, " Synthesis of Power Efficient Multitone Signals with Flat Amplitude Spectrum" *IEEE transactions on communications, vol. 39, No. 7, pp. 1031-1033, July 1991.*

11. Hideki Ochiai and Hideki Imai, "OFDM-CDMA with Peak Power Reduction Based on the Spreading Sequences" *IEEE International Conference on Communications, vol. 3, pp. 1299-1303, June 1998.*

12. Kaiser,Stefan, "OFDM-CDMA versus DS-CDMA: performance evaluation for fading channels", *IEEE International Conference on Communications, pp. 1722-1726, Jun. 1995.*

13. R.W.Chang, "Orthogonal frequency division multiplexing,", *U.S. Patent 3,488,445, filed 1996, issued Jan.6, 1970.*

14. Dinis, Rui, Gusmao, Antonio,"Performance evaluation of a multicarrier modulation technique allowing strongly nonlinear amplification", *IEEE International Conference on Communications, vol. 2, Jun. 1998.*

15. Fazel, K.; Kaiser, S., "Analysis of non-linear distortions on MC-CDMA", *IEEE International Conference on Communications, vol. 2, pp. 1028-1034, Jun 1998.*

16. Tellambura, C., "Coding technique for reducing peak-to-average power ratio in OFDM", *IEEE Global Telecommunications Conference, vol. 5, pp. 2783-2787, Nov. 1998.*

17. Miller, Scott L., O'Dea, Robert J. "Peak power and bandwidth efficient linear modulation", *IEEE Transactions on Communications, vol. 46, pp. 1639-1648, Dec. 1998.*

18. Schilpp, M.; Sauer-Greff, W.; Rupprecht, W.; Bogenfeld, E., "Influence of oscillator phase noise and clipping on OFDM for terrestrial broadcasting of digital HDTV", *IEEE International Conference on Communications, pp. 1678-1682, Jun. 1995.*

19. Van Lint, J.H., Introduction to Coding theory, *Springer-Verlag, Berlin, 2nd ed., 1992.*

20. W.W. Peterson and E.J. Weldon Jr., Error-correcting Codes, *2nd Ed., Cambridge, MA : MIT, 1972.*

21. D.Wulich, "Reduction of peak to mean ratio of multicarrier modulation using cyclic coding" *Electronics Letters, vol. 32, pp. 432-433, 1996.*

22. Yunjun Zhang, Abbas Yongacoglu, Jean-Yves Chouinard and Liang Zhang, "OFDM peak power reduction by sub-block-coding and its extended versions" *IEEE Vehicular Technology Conference, vol. 1, pp. 695-699, May 1999.*

23. J.G. Proakis, Digital communications, *Mc-Graw Hill, New York, NY, U.S.A., 3rd ed., 1995.*

24. W.C.Jakes, Jr., Microwave Mobile Communications, *New York, NY, U.S.A, John Wiley and Sons, 1974.*

25. Lupas, Ruxandra; Verdu, Sergio, "Linear multiuser detectors for synchronous code-division multiple-access channels", *IEEE Transactions on Information Theory, pp. 123-136, 1989.*